Acknowledgement

A big thank to all the people who made this work possible.

Our supervisor,Dr.**OUADI Abderrahmane** who was with us in every single moment, from the starting of the project until its accomplishment. he provides us inspiration, encouragement and good company.

Also We want to thanks all the teachers who gave us all the skills that we need to succeed.

At the end, and most importantly, We wish to thank our parents. They raised us, support us, taught us and love us. To them We wish a long life.

Dedication

This work is dedicated to:

The sake of Allah, my Creator and my Master, for helping and guiding me through all the way And the Messenger of God, Muhammad al-Mustafa, may God's prayers and peace be upon him,

My beloved,precious and valuable mother,father and brothers. I would like to thank you so much for your support and sacrifices and may God make your destiny a paradise of Eden,

My friends and classmates who supported me throughout the process,

Nassim

Dedication

This work is dedicated to:

First and foremost, to God Almighty, my creator, my source of inspiration, wisdom, knowledge, and understanding.

To my beloved parents, without your support, guidance, sacrifices, prayers, endless love and encouragement, I would never have been able to achieve my goals. I thank you from the depths of my heart for making me the person I am today. may God make your destiny a paradise of Eden.

To my beloved siblings, my whole family. May Allah bless you all.

To my friends and mates, thank you for your endless motivation, help and support.

Imad eddine

Abstract

Synchrophasor technology has made it possible to continually check on the condition of power system networks in the Wide Area Measurement System (WAMS) and more recently in the distribution section (which needs more phasor measurement units accuracy and precision). The phasor measurement unit can be used either as a standalone device for simple measurements or as multiple ones that are spread out geographically (small and wide area) and play a significant role in measerement(Wide Area Measerement System) , control (Wide Area Suppelemntary Conrol) and protection (Wide Area Protection) of the power system networks in real time as well as providing time-stamped measurements of voltage and current phasors in just microseconds. to keep the healthy and fault-free power system network in place. Phasor measurement units may employ the Discrete Fourier Transform (DFT) some in classical pmu(P-class) which may be improved to satisfy the requirements accuracy in the IEEE.standard c37-118to estimate the phasor. In this project, the sampling rate and quantization resolution effect have been included in our measurement algorithm. These parameters have been increased and simulated, and the obtained results show improvements in the requested accuracy.

Contents

List of Figures

Nomenclature

ADC Analog to Digital Converter

CPU Central Processing Unit

DFT The discrete Fourier transform

DSDR Digital System Disturbance Recorder

FACTS Flexible AC Transmission System

FE Frequency Error

GPS Global Positioning System

ID Identity Document

IEC International Electrotechnical Commission

IED Intelligent Electronic Device

IEEE Institute of Electrical and Electronics Engineers

IOT Internet Of Things

IP Internet protocol

PDC Phasor Data Concentrator

PMU Pasor Measurement unit

PPS Pulse Per Second

PU Per Unit

RFE Rate of Frequency Error

RMS Root Mean Square

$ROCOF$ Rate Of Change Of Frequency

RS Recommended Standard

SOC Second Of Century

TVE Total Vector Error

UTC Coordinated Universal Time

SDFT Smart Discrete Fourier Transform

General Introduction

In recent decades, the use of electrical power has remarkably increased thanks to massive technological development. The major systems are based on this power (such as heating and cooling systems, hospitals, health fields, industrial fields,research centers and dozens of other systems). For that reason, huge power systems have been constructed to cover the demand for this kind of energy. Unfortunately, the wider the power system is, the greater the number of faults and failures will increase (caused by natural phenomena or by the deterioration of transmission lines or any other part of the system). If the protection devices did not detect the fault quickly, the faulty element will be damaged and lose its synchronisation. It is also possible that the damage affects the other healthy elements. For that, a great amount of money has been spent in order to develop protection and control techniques.

The protection technique consists of detection and isolation of the fault. The first task needs to estimate voltage and current phasors. Traditional techniques were able only to do steady estimation because of the absence of synchronization. By the availability of global Positioning System (GPS), phasor measurement unit(PMU) has become the major choice for electric power systems (either for transport or distribution).It can provide voltage and current measurements synchronized to within a microsecond, it is able also to measure all the parameters such as frequency, frequency error, etc. In WAMS, multiple PMU devices are used with the same time reference. By adding a central controller and a high-accuracy communication system, the detection of faults will be done quickly. In such a manner, the power system is well protected and all damage will be avoided.

Chapter 1

Overview on PMU

1.1 Introduction

Phasor measurement unit (PMU) is defined as a device that produces synchronized phasor, frequency, and rate of change of frequency (ROCOF) estimates from voltage and/or current signals and a time-synchronizing signal. [1]

In other words, PMUs are devices that have the capability of estimating phasor values from electrical waveforms. The main task of PMU is to collect phasor data from many locations and display it on the same phasor diagram. With the use of a GPS satellite navigation system, the measurements acquired from all locations are synchronized to a common time base. PMU measurements from various sites are sent to a Phasor Data Concentrator (PDC), which is defined as "a device that integrates data from multiple measuring units". It should be noted that data is processed by the PDC and displayed to users via a user interface, as well as stored in a database for future use.The whole process is called the wide area measurement system. Figure 1.1 shows the block diagram of standard WAMS.

After years of testing, PMU has proved its effectiveness and accuracy; as a result, it has become irreplaceable, especially since the world is moving steadily toward smarter grids that require synchronization and maximum efficiency to represent the current status of the electrical system. This chapter covers synchronization definitions, PMU properties and its primary hardware components.

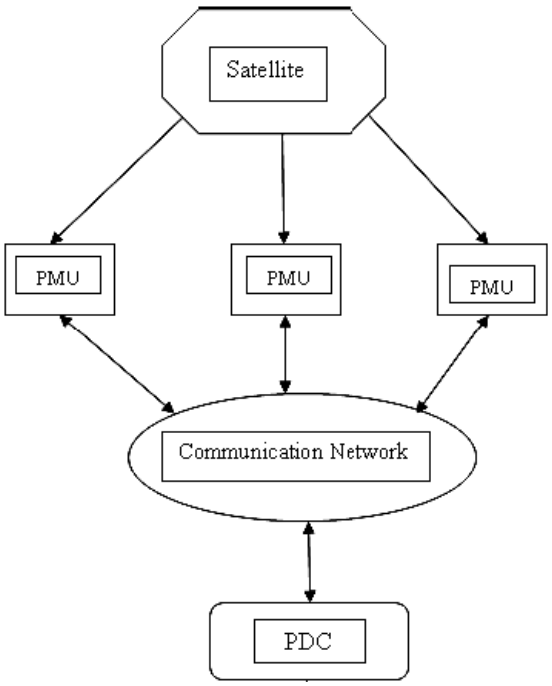

Figure 1.1: General WAMS architecture.

1.2 Definition of Synchrophasor Measurement:

Algorithms for estimation of system states (voltage and current amplitude and phase angle)[2].

1.2.1 Phasor

A phasor is defined as a complex number that represents both the magnitude and phase angle of a sine wave quantity. [3] .

1.2.2 Synchrophasor

A Synchrophasor is a phasor that is time-stamped to an extremely accurate time-reference like GPS signals. Phasors are measured at high speed, typically between 25/30 and 100/120 measurements per second. The IEEE Std. C37.118.2018 defines the synchrophasor representation (X) of a periodic signal as:

$$X(t) = X_m cos(\omega t + \theta) \tag{1.1}$$

$$X = \frac{X_m}{\sqrt{2}} e^{j\theta} \tag{1.2}$$

where the magnitude of the synchrophasor ($| X | = \frac{X_m}{\sqrt{2}}$) is the RMS value of x(t), and $\theta = angle(X)$ represents the momentary phase angle relative to a cosine function at the nominal system frequency synchronized to UTC .[3]

In real-world cases, a sinusoid waveform is not always pure and stationary; it is often distorted by the presence of harmonics, and its frequency may vary. A synchrophasor is defined as a phasor tagged with a common, reliable, and unique time stamp, at intervals that are multiples of the nominal power system frequency.

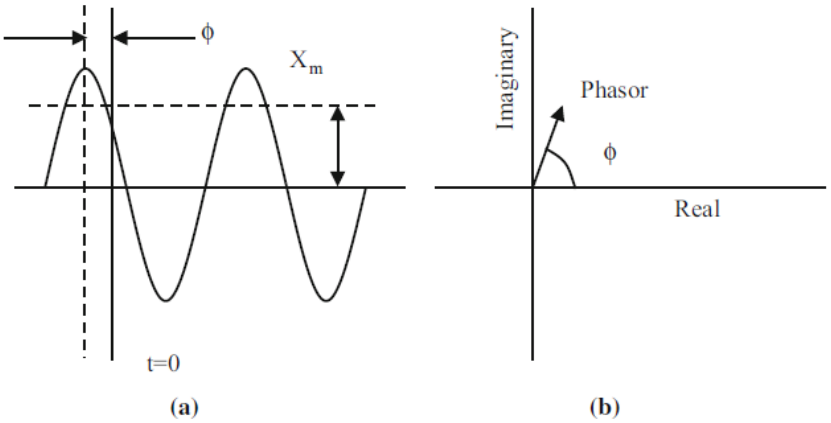

Figure 1.2: A sinusoid (a) and its representation as a phasor (b).

The phase angle of the phasor is arbitrary, as it depends upon the choice of the axis t = 0. Note that the length of the phasor is equal to the RMS value of the sinusoid.

The phase angle differences between two sets of phasor measurements (i.e. d1-d2) is independent of the reference. Typically, one of the phasor measurements is chosen as the

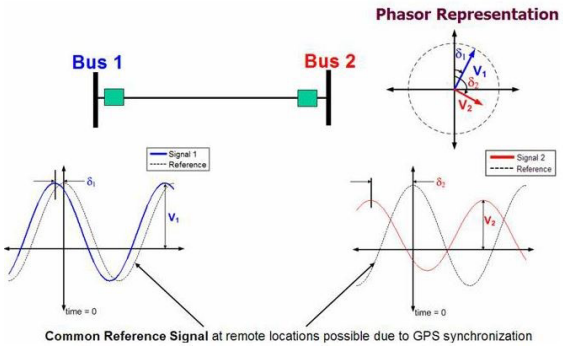

Figure 1.3: Phasor Comparison of Two Different Buses at Remote Location.

reference" and the difference between all the other phase angle measurements (also known as the absolute phase angle) and this common reference" angle is computed and referred to as the relative phase angles with respect to the chosen reference (see figure 1.4) [4]

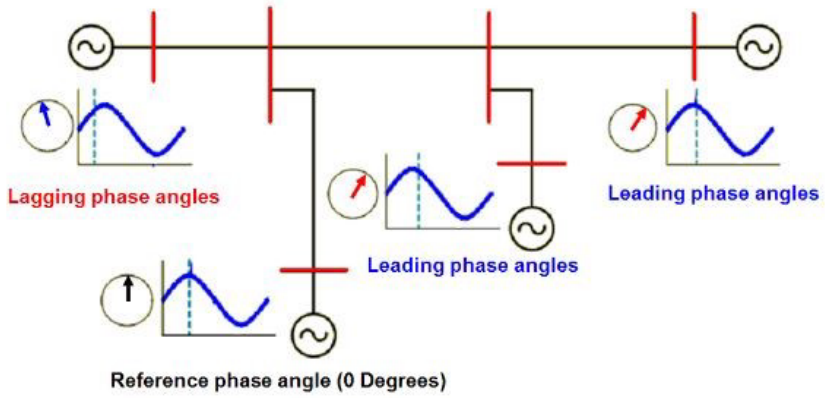

Figure 1.4: Phasor Comparison with Reference Phase angle.

By synchronizing the sampling processes for different signals, which may be hundreds of miles apart, it is possible to put their phasors on the same phasor diagram.

1.2.3 Synchronized Phasors:

Synchronization is achieved by using a highly accurate sampling clock which is phase-locked to the one-pulse-persecond signal provided by a GPS receiver.

Figure 1.5 illustrates the phase angle/UTC time-relationship. If the peak of the measured waveform coincides with the Pulse Per Second; PPS signal as shown in the first case, the phase difference is zero. While in the second case, the phase difference is -90°, the positive zero crossing occurs at the UTC second rollover (sine waveform).

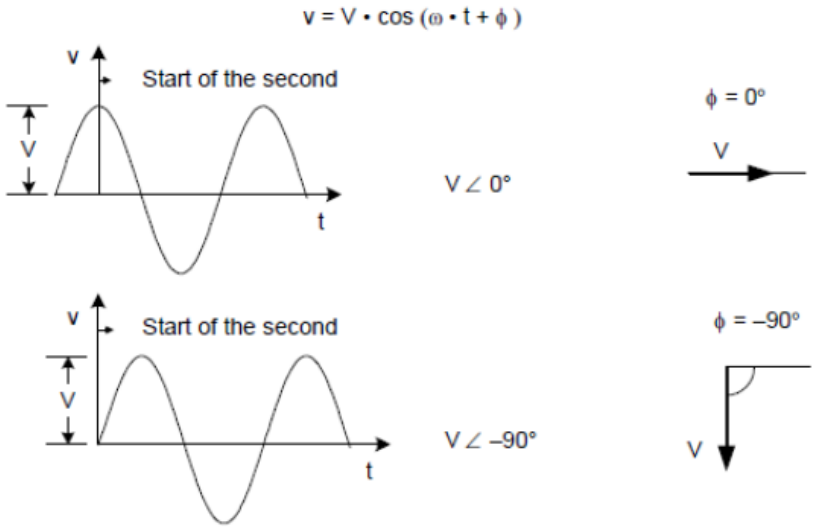

Figure 1.5: Convention for the Synchrophasor Representation.

1.3 PMU history

In power systems, it is well known that active power is nearly proportional to the angle difference between voltages at the two terminals of the transmission line. For that, electrical engineers have always tried to improve the accuracy of those signal angles.

In the early 1980s, the first modern applications of measurements were reported in three papers (Measurement of bus voltage angle between Montreal and Sept-Iles; Dynamic measurement of the absolute voltage angle on long transmission lines; Phase angle measurements with synchronized clocks—Principles and applications.) based on LORAN-C, GOES satellite transmissions in order to obtain synchronization of reference time. With some measurement improvements, engineers were able to estimate the angle between the voltages in two different locations according to the same time reference . The measurement accuracy achieved in these systems was of the order of 40 micro-second, but unfortunately, no attempt was made to measure the voltage phasor magnitude, nor was any account taken of the harmonics contained in the voltage waveform. Taking that into account, these techniques were not suitable for wide area measurement systems and they are no longer in use.

In 1983,Phadke A. G., Thorp, J. S., and Adamiak, M. G. published the first paper [5] discussing the importance of voltage and current phasors, including their parameters and applications, and this paper was the starting point of modern synchronized phasor measurement technology. At that time Global positioning system has proved its efficiency as a reference for wide area systems synchronization, as a conclusion of this researches the

first modern phasor measurement units (PMUs) device using GPS were built at Virginia Tech as shown in Figure 1.6, where (a) and (b) represents two of its prototypes . This PMU was used only at a few substations as an experimental edition. In 1991, the first commercial manufacturing of PMUs was built by Virginia Tech collaboration and Macrodyne. In the same year, IEEE published a standard governing the format of data files created and transmitted by the PMU(multiple revised versions of this standard were published later as it is mentioned in this chapter).

It can be said now that finally the technology of synchronized phasor measurements has come of age, and most modern power systems around the world are in the process of installing wide-area measurement systems consisting of the phasor measurement units. (based on [6]).

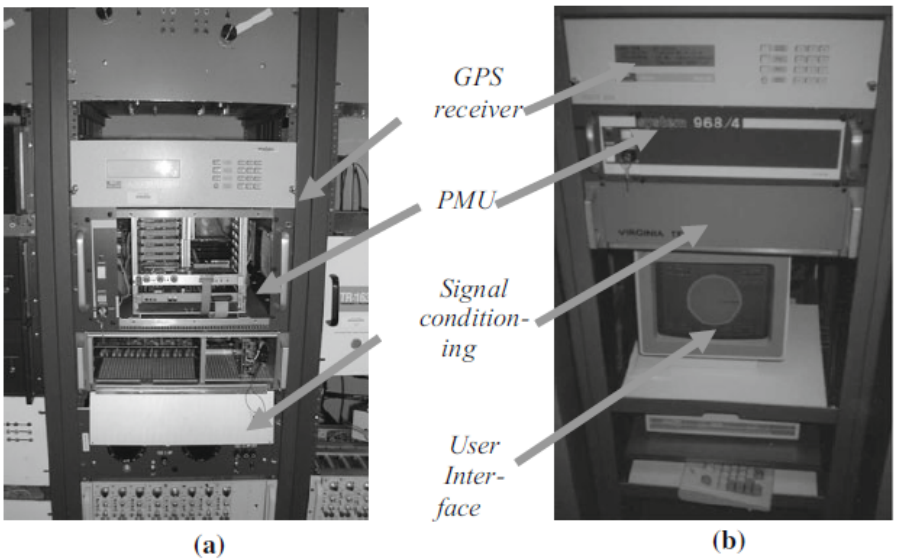

Figure 1.6: The first PMU built at the power systems research laboratory at Virginia Tech. (a) is the first prototype; (b) is the second prototype[6]

1.4 PMU applications

As it is mentioned in the previous clause, synchrophasor measurements usig PMUs is relatively a new technology. many researches are countineously done for the improvement of this technology because of its effectiveness in electrical domain and its multiple applications in power systems which are described as follows:

- A. Early Application:
  PMU at early stage worked as digital system disturbance recorder (DSDRs) due to limitation in availability and bandwidth of communication channel.

- B. Power system protection:
  One of the main applications of PMUs is the involving in Power system protection technique by its ability to detect and isolate different faults that occur in any part of the system .

- C. State Estimation
  Nowadays, power systems' control centers use all the data received from different PMUs (phase angles, signal magnitude, active and reactive power, frequency, frequency error...etc) in order to monitor the state of the system with the help of some other estimation procedure.

- D. Power system control:
  Basically, Flexible AC transmission system devices (FACTS) are used for system controllability. But the control objective also depends on the remote signal occurrence, which can be done using synchrophasors. So the addition of a PMU device to the local controller will increase the overall robustness of the power system. (based on [7])

1.5 PMU hardware

The different manufactured phasor measurement units have many differences in their parts, which makes it difficult to discuss their hardware parts in a general way. However, it is possible to discuss the basic edition of this device that contains its main parts. Figure1.7 shows the elements that must be included in any PMU device. Analog inputs are voltages and currents obtained from transforms that are going to be converted to digital values (machine readable values) after matching the A/D converter requirements. In the same time, the GPS receiver is providing the PPS needed for synchronization. The last stage is the estimation of

phasors by the processor and transmitting them using a communication system.
The next passage discusses major PMU elements, particularly:

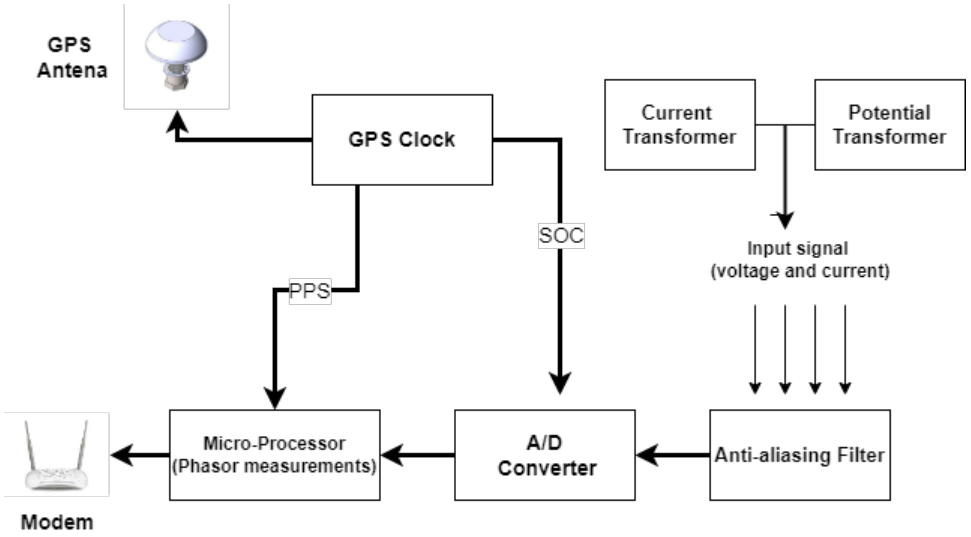

Figure 1.7: Major elements of modern phasor measurement unit.

1.5.1 Input signals sensing

The analog block input variables such as voltages and currents are electrically isolated from power system transducers. Besides the electrical isolation, the measured input signals are scaled down from the power system intensities to levels suitable for data acquisition systems.

- Current sensing :
  Since the analog to digital A/D converter accepts only voltage signals, the measured currents are converted to equivalent voltages using a current-to-voltage converter. The current measurement signal obtained from a current transformer is reduced to a lower level by an auxiliary current transformer. The second internal circuit by using galvanic isolation input transformers. The current 1A or 5A rated is conditioned and converted to its representation.

- Voltage sensing:
  The voltage measurement is first performed through a potential transformer and then supplied to an auxiliary potential transformer that reduces the voltage level. A voltage signal conditioning circuit is used to further reduce this voltage to a suitable level for the next stage[8].

Since the range of ±5 is required for the A/D converter module, it is necessary to build up a conditioning circuit in order to transform the real values of the input signals to the required range of the A/D converter.

1.5.2 Anti-aliasing filter

The input signal of PMU may contain components with a high frequency. These components may damage the flatness of the signal. For that, it is necessary to remove them using an anti-aliasing filter which has a cut-off frequency of less than one-half of the sampling rate frequency (it is known as the "nyquist frequency"). For example, if the sampling rate is fixed at 1.8 kHz,it is recommended to choose a 500–800 Hz cut-off frequency for the anti-aliasing filter .

1.5.2.1 Butterworth Filter

The Butterworth low-pass filter has the highest passband flatness. As a result, a Butterworth low-pass filter is frequently utilized as an anti-aliasing filter in data converter applications where accurate signal levels over the whole passband are required.[9].These filters are distinguished by the fact that their magnitude response is flat in the passband. This indicates that the first (2N-1) derivatives of the magnitude-squared function are zero at $\Omega = O$ for a Nth-order lowpass filter. Another feature is that the magnitude response in the passband and stopband is monotone. For a continuous-time Butterworth lowpass filter, the magnitude-squared function is as follows:

$$\left|H_c(j\Omega)\right|^2 = \frac{1}{1+\left(\frac{j\Omega}{j\Omega_c}\right)^{2N}} \tag{1.3}$$

With:
N: the order of the filter.
Ω_c: the cut-off frequency.
Ω : the operating frequency
The function is plotted in Figure 1.8

As the parameter N in Eq 1.3 increases, the filter characteristics become sharper: that is why they remain close to unity over more of the passband and become close to zero more rapidly in the stopband, although the magnitude-squared function at the cutoff frequency Ωc will always be equal to one-half because of the nature of Eq 1.3 [9], The dependence of the Butterworth filter characteristic on the parameter N is indicated in Figure 1.9.

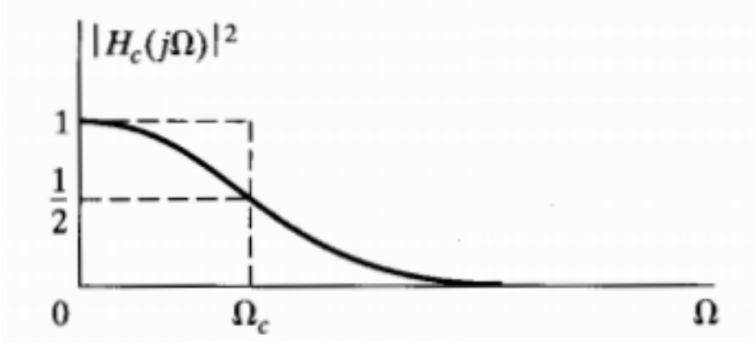

Figure 1.8: Magnitude squared function for continuous-time Butterworth Filter[9].

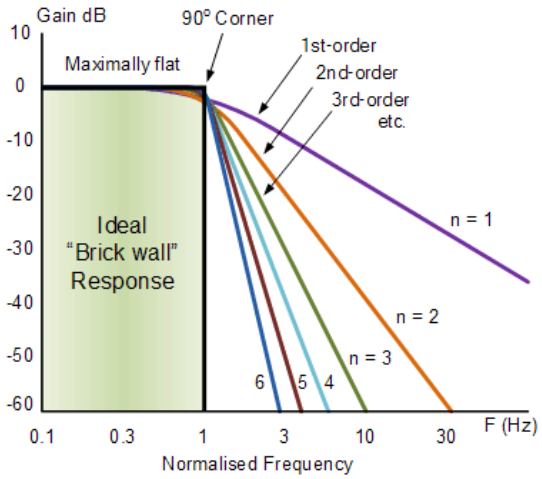

Figure 1.9: Dependence of Butterworth gain characteristics on the order N.

Group delay

In addition to the amplitude response discussed above, the anti-aliasing filter has a phase response $\phi(j\omega)$. This is significant since it contributes to the system under control's delays. This contribution represents a group delay, which is defined as:

$$\tau_g(j\omega) = \frac{d(\phi(j\omega))}{d\omega} \tag{1.4}$$

The group delay characteristics of butterwoth filter response are reasonably uniform at low frequencies, and the magnitude of the group delay in this region is approximately 0.5/fc seconds[10], so for a 500 Hz cut-off frequency. This phase shift must be taken into account for better phasor estimation precision.

1.5.3 Analog-to-digital converter

Analog-to-digital (A/D) and digital-to-analog (D/A) converters, often known as data converters, serve an important function as connectors between the real analog world and digital technology. They are currently essential in sensor networks, the internet of things (IoT), robotics, and self-driving cars, as well as high-precision instrumentation and wideband communication systems. As the world becomes more reliant on digital information processing, the relevance of data converters grows.[11]
The basic ADC device shown in Figure 1.5.3 consists of two parts. The first stage performs a sample - and - hold operation that physically converts an analog signal x(t) into a discrete - time signal x[k]. The second stage consists of a quantizer that maps the discrete - time sample value x[k] into an equivalent digital word $X_D[k]$. An n - bit ADC quantizes x [k] into one of 2^n possible digital values[12].

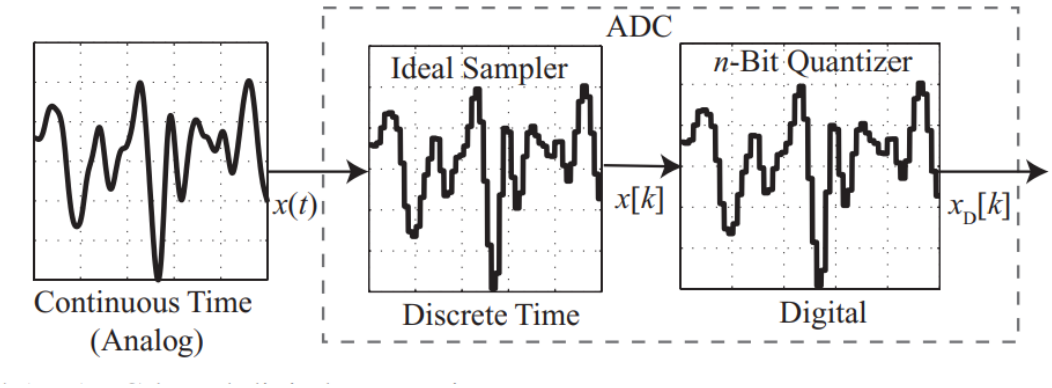

Figure 1.10: ADC - based digital conversion system [12].

1.5.4 Global posisioning system

The Global Positioning System (GPS) was initiated with the launch of the first Block I satellites in 1978 by the US Department of Defense. By 1994, the entire constellation of 24 contemporary satellites had been deployed. (There are 30 active satellites in orbit in 2007, with the extra satellites offering more accuracy in estimating the spatial coordinates of the receivers.) The Block I and II satellites have been decommissioned.) These are grouped into six orbital planes separated by 60 degrees and inclined by around 55 degrees with regard to the equatorial plane (see Fig1.11).

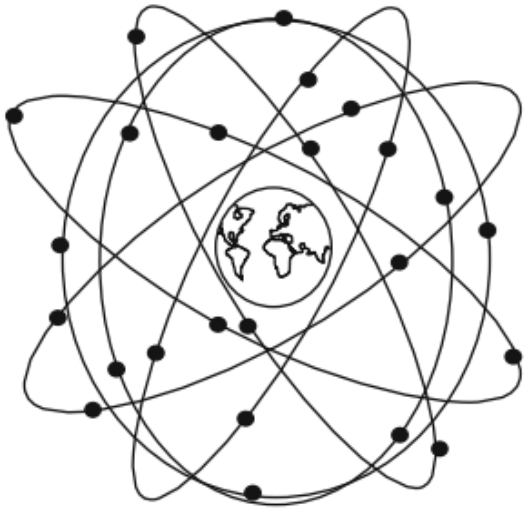

Figure 1.11: Representation of the GPS satellite disposition [6].

The GPS signal is most commonly used to determine the coordinates of the receiver. However, with a phasor monitoring unit, the signal that is most relevant is one pulse per second. This pulse, as received by any receiver on Earth, is 1 microsecond apart from all other received pulses. In practice, synchronization accuracies of the order of a few hundred nanoseconds have been achieved.

GPS satellites use precise clocks to transmit a single pulse-per-second signal. GPS time does not take into account earth's rotation because GPS receivers themselves correct the GPS time to account for this difference (leap-second correction) so that the receivers report UTC clock time. The pulse's identity is defined by the number of seconds since the clocks began to count (January 6, 1980). It should be noted that the PMU Standard uses a UNIX time base with a second-of-century (SOC) counter that began counting on January 1, 1970, at midnight.[6]

1.5.5 Central processing unit

CPU is a combination of of hardware components and software functions that make the operating of IEDs(include protective device and PMU) successfully done. The CPU performs its operations either as one unit with multi-core processors or by splitting it into four units working as sub-CPUs (front-end CPU, main CPU, logic CPU, and communication CPU). The main purpose of software functions is to measure the phasor of current and voltage signals using the approaches discussed in Chapter 2. Other estimations of interest include the frequency and rate of change of frequency recorded locally, which are also included in

the PMU output data.

1.6 Communication

For the communication section, if the PMU is used only for phasors' recording without any data transmission, there is no need for this no need for this block. Otherwise, It must be inserted properly with respect to IEEE standards protocol.

1.6.1 Message application

For PMU needs, any communication system can be used for data transmission, either by using protocol stack (Internet protocol(IP)for example) or by using more direct system (Ethernet,RS-232); in both cases, the message frames must be sent well arranged as it is defined.
This message protocol may be used for communication with a single PMU or a secondary system that receives data from several PMUs (which is called a phasor data concentrator). In second case, data frames should include PDC ID same as for each phasor in order to reach accurate interpretation of measured data.[13]

1.6.2 Communication format

For any communication system, there are mainly four types of messages described as follows:

- Configuration frames: machine-readable messages describing either present or maximum device configuration are sent to the PDC on demand (informational data)or automatically(measured and computed data). It is sent only when a configuration change of the PMU has happened.
- Header frame: barely similar to a configuration message, it contains descriptive information with a human-readable message type.
- Command frame : machine-readable codes sent from the PDC to the PMU for both control(resume or stop transmission) and request configuration .
- Data frames : are the measurements taken by the PMU. They are continuously sent to the PDC.[13]

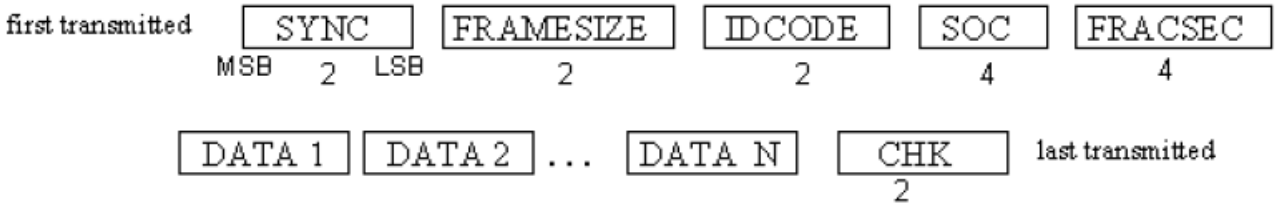

Figure 1.12: standard frame format

All types of messages have the same frame format shown in the figure. 1.12
As an example, the table below (1.1) describes in detail the data frame format.

Field	Description	Size (Bytes)
SYNC	Synchronization and Frame Format Field	2
FRAMESIZE	Total number of bytes in this frame.	2
IDCODE	PMU/DC ID number	2
SOC	Second count (UNIX time, starting midnight 01-Jan-1970 neglecting leap seconds).	4
FRACSEC	Time of phasor measurement in microseconds with Time Quality	4
STAT	Bitmapped flags: Data valid?, PMU OK?, PMU sync?, Data align by time?, PMU Trigger?,	2
PHASORS	Phasor data, 16-bit integer, rectangular format. The first two bytes contain the real part of the phasor and the second two contain the imaginary part.	16
FREQ	16-bit signed integer. Frequency deviation from nominal in millihertz.	2
DFREQ	Rate of change of frequency	2
ANALOG	32-bit floating point	12
DIGITAL	Digital data, 16-bit fields	2
CHK	CRC-CCITT	2

]

Table 1.1: Data message example[13]

1.7 Protection of Power Systems

PMUs are commonly used for protection purposes in wide area measurement systems (WAMS) as well as for distribution sections. PMUs are commonly used for protection purposes. That's done by the existence of a central controller, which claims data from all devices and then calculates the total fault currents. According to Kirchhoff's law, the total amount must equal zero. Otherwise, the system is facing a fault in one of its parts, which leads to disconnecting that part in order to protect the whole system(the system can be faulty even though Kirchhoff's law is verified) .

The figure 1.13 below represents a sample micro-grid installation with a modern protection system. Three types of faults may occur in this electrical system, and they can be distinguished and isolated as follows:

- Internal fault: The fault is on the feeder, and the feeder should be disconnected from the grid and all the micro-sources should be opened.
- External fault :The sum of fault currents is equal to zero but the PMU installed next to the Point Common Coupling measures a very high current. In this case, the main circuit breaker (connection to the utility-grid) should be tripped.
- Lateral fault : as the previous case the sum of fault currents is equal to zero; however, the currents that passed through the faulty micro-source is much higher than the maximum short circuit current of that micro-source, hence the faulty lateral would be identified and the tripping command is sent to the related circuit breaker.

1.8 IEC/IEEE PMU standards

- **About the IEC**

  The International Electrotechnical Commission (IEC) is the leading global organization that prepares and publishes International Standards for all electrical, electronic and related technologies.

- **About the IEEE**

  IEEE is the world's largest professional association dedicated to advancing technological innovation and excellence for the benefit of humanity. IEEE and its members inspire a global community through their highly cited publications, conferences, technology standards, and professional and educational activities.

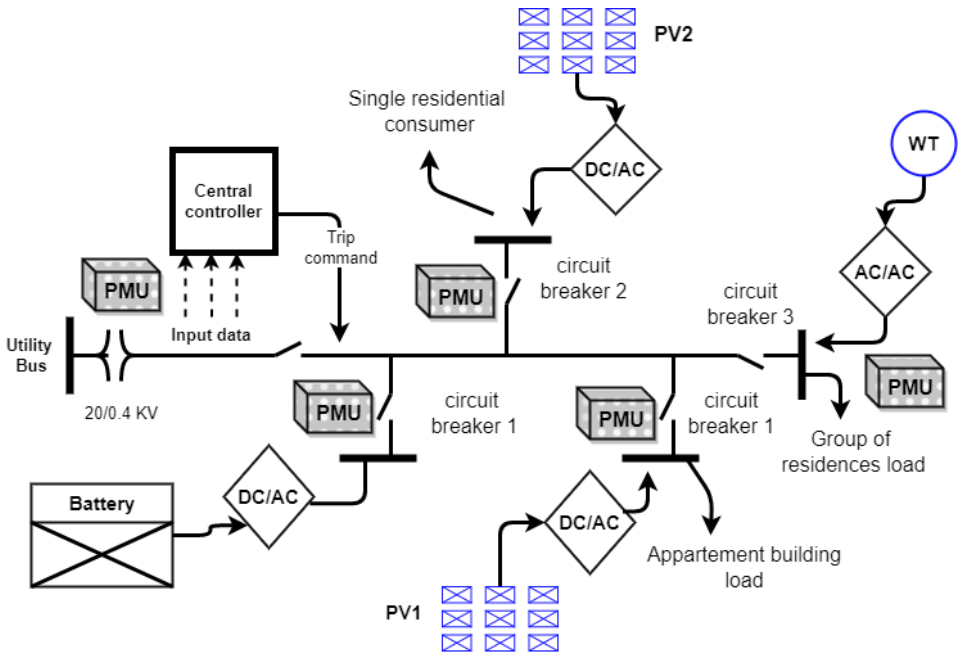

Figure 1.13: Sample micro-grid with PMUs and central controller.

1.8.0.1 IEC/IEEE 60255-118-1:2018

This document provides continuation and further development of previous synchrophasor standards, notably the IEEE C37.118 series. It defines synchrophasor, frequency, and rate of change of frequency (ROCOF) measurements as used in this technology. These definitions are in agreement with most research on and analysis of dynamic electric power systems, but may differ from those given in other contexts. Function and performance requirements are given for synchrophasor measurements. Tests, evaluation criteria, and error limits are provided to determine compliance with the requirements.[14] IEC/IEEE 60255-118-1 standards mainly consist of:

- Definitions and abbreviation of the well-known terms in this domain.
- Synchrophasor and its quantities measurements.
- Measurement evaluation:
  PMU performance shall be determined by comparing the measured values with the reference values using the TVE, FE, and RFE formulas.
- Measurement compliance test and evaluation:
  in this clause IEC/IEEE researchers precised the the values that should be taken as a reference either for the quantities or for the errors that should not be exceeded for both

steady and dynamic states and we'll apply all of these in measurement tests included in chapter 2.

- Documentation shall be provided by any vendor claiming compliance with this document that shall include the following information:
  - a) performance class;
  - b) measurements that meet this class of performance;
  - c) selectable reporting rates;
  - d) nominal voltage and current magnitudes;
  - e) input(s) used for the frequency and ROCOF measurements;
  - f) PMU settings;
  - g) test results demonstrating performance;
  - h) test equipment description;
  - i) environmental conditions during the testing.

Chapter 2

DFT measurement algorithm: Analysis and and testing

2.1 Introduction

The input signals need to be converted from analog to digital, that may result in some errors A PMU measures 50/60 Hz AC voltage and/or current signals to provide phasor and frequency measurements. The analog AC waveforms are digitized by an analog to digital converter, as shown in Fig. 1.7 in the previous chapter , that may cause a small error in the resulting output. This chapter presents the different estimation techniques used , the way of extracting phasors of a sinusoidal signal, and the different results obtained from evaluating the pmu in both the steady state and dynamic conditions.

2.1.1 DFT estimation technique:

The discrete Fourier transform (DFT) is one of the most efficient techniques in digital computation. It is now at the heart of a lot of digital signal processing systems. It converts the time domain to the frequency domain keeping all the information carried by the input signal unchangeable .

Consider a sinusoidal input signal of frequency f_o given by:

$$X(t) = X_m cos(2\pi f_0 t + \phi_i). \tag{2.1}$$

Where:
X_m : maximum value of the input signal,
f_0: the nominal frequency,

ϕ_i : the initial phase angle of the input signal
The signal is conventionally represented by a phasor related to the fundamental frequency component of its DFT $\bar{X}$

$$\bar{X} = \frac{X_m}{\sqrt{2}} e^{j\phi} \tag{2.2}$$

$$\bar{X} = X cos\phi + jX sin\phi \tag{2.3}$$

Assuming that the signal x(t) is sampled N times per fundamental period (50Hz or 60Hz) waveform to generate the sample set:

$$x_k = X_m cos(\frac{2\pi k}{N f_0} + \phi_i) \tag{2.4}$$

where the phasor is given by:

$$\bar{X} = \frac{\sqrt{2}}{N}(X_c - jX_s) \tag{2.5}$$

where:

$$X_c = \sum_{k=1}^{N} X_k cos(\frac{2\pi}{N} k) \tag{2.6}$$

and :

$$X_s = \sum_{k=1}^{N} X_k sin(\frac{2\pi}{N} k) \tag{2.7}$$

In some literature, the definition of DFT with no harmonics is given by:

$$X = \frac{\sqrt{2}}{N} \sum_{k=1}^{N} X_k e^{-j\frac{2\pi}{N}k} \tag{2.8}$$

DFT has two types of estimation techniques . These types are recursive and non-recursive DFT.

2.1.1.1 Non-recursive DFT:

Equation 2.8 represents a phasor measurement performed by the DFT algorithm for a period data window that is a set of N samples for a fixed data window. This DFT procedure provides the phasor computation for a fixed-length data window, but Eq. 2.8 represents non-recursive estimations. This means that Eq. 2.8 calculations are repeated for each data window as shown in Figure.2.1 as time progresses. This procedure requires 2N multiplications and (N-l) additions to produce the phasor X. It should, however, be noted that in progressing from one data window to the next, only one sample (X) is discarded and only one sample (X_N) is added to the data set. [8].

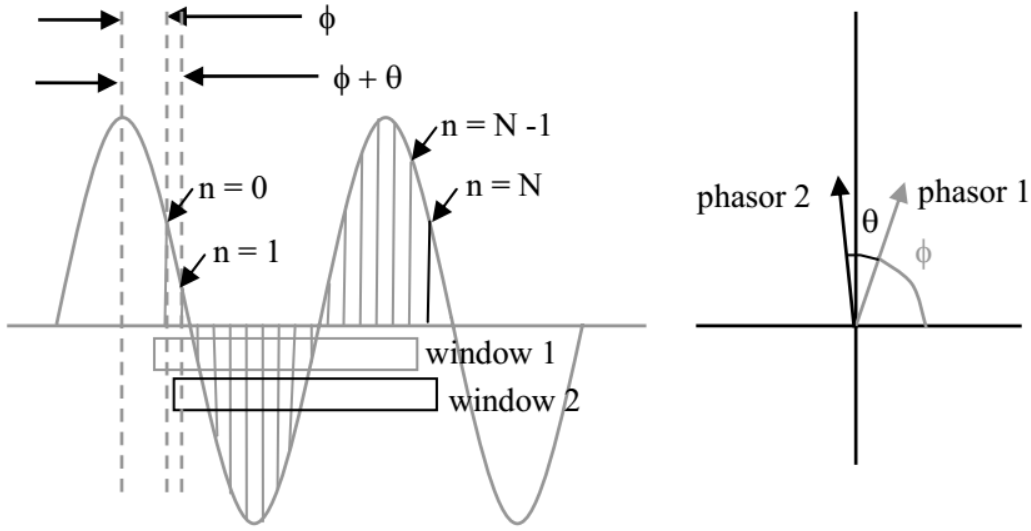

Figure 2.1: Non-recursive phasor estimation for two windows[8].

2.1.1.2 Recursive algorithm:

A modified algorithm which saves computation taking into account data from previous window is called as recursive algorithm ,in which the phasor is calculated for X_{N-1} and it is updated recursively to calculate the next phasor (X_N)which can be given by equation 2.10:

$$\hat{X}_N = \frac{\sqrt{2}}{N} \sum_{k=0}^{N-1} X_{k+1} e^{-j\frac{2\pi}{N}(k+1)} \tag{2.9}$$

$$\hat{X}_N = \hat{X}_{N-1} + \frac{\sqrt{2}}{N}(x_N - x_0) e^{-j\frac{2\pi}{N}0} \tag{2.10}$$

where

$$e^{-j\frac{2\pi}{N}0} = e^{-j\frac{2\pi}{N}N} \tag{2.11}$$

since N samples span exactly one period of the fundamental frequency. if the last sample of the recursive estimate is (N+r), the recursive DFT method is given by the equation2.12:

$$\hat{X}_{N+r} = \hat{X}_{N+r-1} + \frac{\sqrt{2}}{N}(x_{N+r} - x_r) e^{-j\frac{2\pi}{N}r} \tag{2.12}$$

The recursive phasor estimation differs from the non-recursive estimate by an angular retardation of $\theta(\frac{2\pi}{N})$. The advantage of using this alternative definition for the phasor from the new data window is that (N – 1) multiplications by the Fourier coefficients in the new window are the same as those used in the first window. Only a recursive update on the old phasor needs to be made to determine the value of the new phasor.[6]

It is interesting to note that when the input signal is a pure sine wave of fundamental frequency $\hat{x}_{N+r} = \hat{x}_r$ for all r as shown in Figure 2.2:

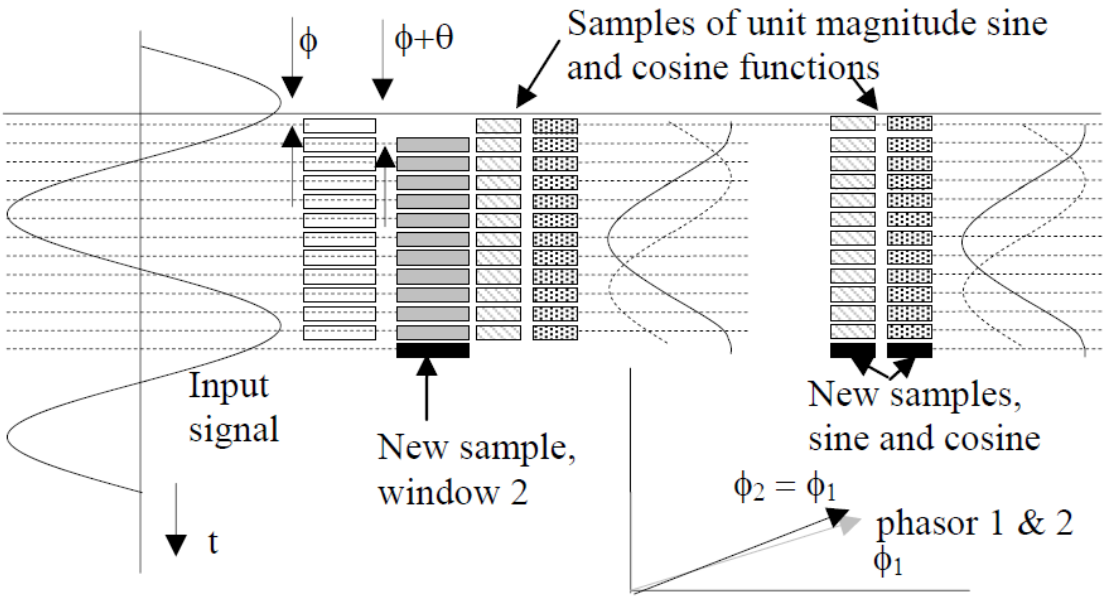

Figure 2.2: recursive phasor estimation for 2 windows.

2.1.2 Frequency tracking algorithm (Smart DFT algorithm)

The DFT phasor computation is faulty when the power system runs at off-nominal frequencies, as is well-documented in the literature [15]. A variety of approaches have been developed to measure the power system frequency, such as the level crossing technique[5] ,which is sensitive to noise, presence of DC components in the signal, and harmonics. Other techniques as Kalman filter technique [16] ,the least square [17], leakage effect technique [18], and phasor-based technique [19, 20]. These techniques are mainly used to measure steady state frequency based on the assumption of a fixed frequency model based on the fixed frequency model assumption. Smart discrete Fourier transform (SDFT) is a digital algorithm that relies on DFT and overcomes faults that arise when frequency offset occurs and keeps all the advantages of the DFT, such as fast calculation and immunity to harmonics of fundamental frequency. Moreover, it overcomes the leakage error and even recursive computing can be used in SDFT.

When there are disturbances in the power system, the sinusoidal frequency f(t) is no longer constant and instead depends on time t. It is possible to express the waveform's sinusoidal signal frequency via a nominal frequency f_0 varying with a frequency deviation Δf . The following equations shortly illustrate the flow of SDFT[21, 22] :

$$x(t) = X_m cos(2\pi(f_0 + \Delta f)t + \phi_i). \tag{2.13}$$

The signal is represented by a phasor $\bar{X}$
:

$$\bar{X} = \frac{X_m}{\sqrt{2}} e^{j(2\pi\Delta f t + \phi)} \tag{2.14}$$

$$\bar{X} = X cos\phi + jX sin\phi \tag{2.15}$$

The sampled signal is then written as :

$$x(k) = X_m cos(2\pi f k(\frac{f_0 + \Delta f}{N f_0}) + \phi) \tag{2.16}$$

Where N is the sampling rate in samples/cycle.
X_m : maximum value of the input signal,
f_0: the nominal frequency,
ϕ_i : the initial phase angle of the input signal

The frequency component in the DFT spectrum of x(k), at the r^{th} sample, is given :

$$\hat{x}_r = \frac{2}{N} \sum_{k=0}^{N-1} x(k+r) e^{-j\frac{2\pi}{N}k} \tag{2.17}$$

by defining the system frequency deviation as Δf:

$$f = f_0 + \Delta f, \tag{2.18}$$

the phasor $\hat{x}_r$ can be obtained as:

$$\hat{x}_r = A_r + B_r \tag{2.19}$$

and defining a as:

$$a = e^{-j\frac{2\pi(f_0+\Delta f)}{N f_0} r} \tag{2.20}$$

by doing some mathematical manipulations and using the following identity ,

$$\sum_{i=0}^{N-1} (e^{j\theta})^i = \frac{sin\frac{N\theta}{2}}{sin\frac{\theta}{2}} e^{(j(N-1)\frac{\theta}{2})} \tag{2.21}$$

we get the following relationship:

$$A_r = \frac{x_m}{N} \frac{sin\frac{\pi\Delta f}{f_0}}{sin\frac{\pi\Delta f}{Nf_0}} e^{2\pi\frac{(f_0+\Delta f)}{Nf_0}+\frac{\pi(N-1)\Delta f}{Nf_0}+\phi} \tag{2.22}$$

and defining w as:

$$w = a + a^{-1} = 2cos(2\pi\frac{(f_0+\Delta f)}{Nf_0}) \tag{2.23}$$

B_r is ignored since Δf is so small,.the frequency deviation Δf is written as :

$$\Delta f = \frac{Nf_0}{2\pi} cos^{-1}\Re(\frac{w}{2}) - f_0 \tag{2.24}$$

and the amplitude X_m and the phase ϕ are determined as:

$$X_m = |A_r| \frac{Nsin\frac{\pi\Delta f}{Nf_0}}{sin\frac{\pi\Delta f}{f_0}} \tag{2.25}$$

$$\phi = angle(A_r) - \frac{\pi(N-1)\Delta f}{Nf_0} \tag{2.26}$$

The derived expressions for the parameters w and A_r are:

$$w = \frac{\hat{x}_r + \hat{x}_{r+2}}{\hat{x}_{r+1}} \tag{2.27}$$

$$A_r = \frac{a\hat{x}_{r+1} - \hat{x}_r}{a^2 - 1} \tag{2.28}$$

Finally, after calculating the values of A_r, and Δf, the value of the estimated SDFT phasor can be obtained.

2.2 The IEEE Std. C37.118 compliance

The only officially recognized PMU standard is the IEEE C37.118. Such a standard derives from a preliminary version of an IEEE standard for synchrophasors, PMU compliance to the IEEE Std. is achieved by satisfying the measurement requirements during both steady state and dynamic compliance. The PMU compliance is assessed by comparing its performance to the IEEE Std. requirements and verifying if they respect the defined limits.

2.2.1 Phasor and frequency measurement algorithms testing:

Algorithms tests are performed with a transient data signal generated from mathematical equations simulating the steady state or transient waveform cases of the power system as specified by the IEEE C37.118 standard[1].

2.2.2 Performance Classes:

The IEEE.std c37-118 [14]has defined two performance classes which correspond to two different PMU applications and compliant requirements:

- P-class is intended for protection applications or any application requiring fast response times and reduced reporting latencies.
- M-class is intended for measurement applications where more importance is given to the accuracy of the PMU estimations and particularly to its capability to reject interharmonics, rather than their response times and reporting latencies.

2.3 Synchrophasor measurement evaluation

The evaluation of the synchrophasor measurement is done with the actual or theoretical value of the synchrophasor and the measured value . The total vector error (TVE) is then determined according to [14]:

$$TVE(n) = \frac{\sqrt{(\hat{X}_r(n) - X_r(n))^2 + (\hat{X}_i(n) - X_i(n))^2}}{\sqrt{(X_r(n))^2 + (X_i(n))^2}} \tag{2.29}$$

where $X(n)$ is the theoretical value or actual synchrophasor , $\hat{X}(n)$ is measured Synchrophasor and r and i identify the real and imaginary parts of the synchrophasor respectively.

It should be noted that the measured phasor might be either a voltage or a current phasor. The ideal, measured, and error phasors are presented graphically in Figure 2.3. Figure 2.3 demonstrates the relationship between TVE, magnitude error, and angle error in the same figure. This figure 2.3 shows the expected TVE with angle errors ranging from -0.5° to 0.5° and magnitude errors ranging from 0, 0.1, 0.2, and 0.3.

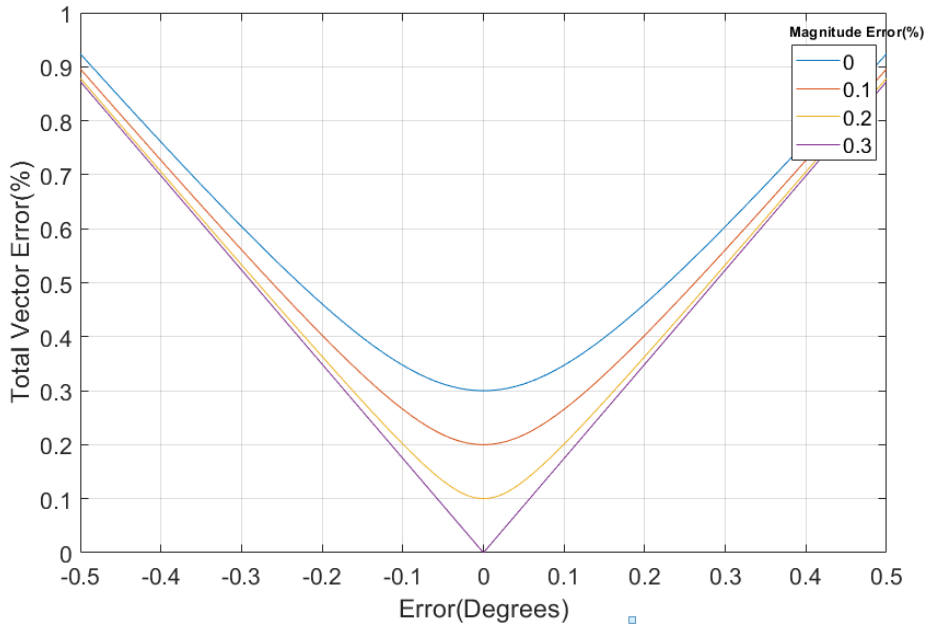

Figure 2.3: TVE in percentage for angle errors of –0.5° to 0.5° and magnitude errors of 0, 0.1, 0.2 and 0.3.

- Frequency and ROCOF measurement evaluation:

Frequency and ROCOF measurements shall be evaluated as the difference between the measured values and the theoretical values .

- Frequency Error

The Frequency Error (FE) is defined in the IEEE Std C37.118 [14] as follows:

$$FE(n) = F_{measured}(n) - F_{ref}(n) \tag{2.30}$$

- ROCOF Error

The ROCOF Error (RFE) is defined in the IEEE Std C37.118 [14] as follows:

$$RFE(n) = (\frac{\mathrm{d}f}{\mathrm{d}t})_{measured}(n) - (\frac{\mathrm{d}f}{\mathrm{d}t})_{ref}(n) \tag{2.31}$$

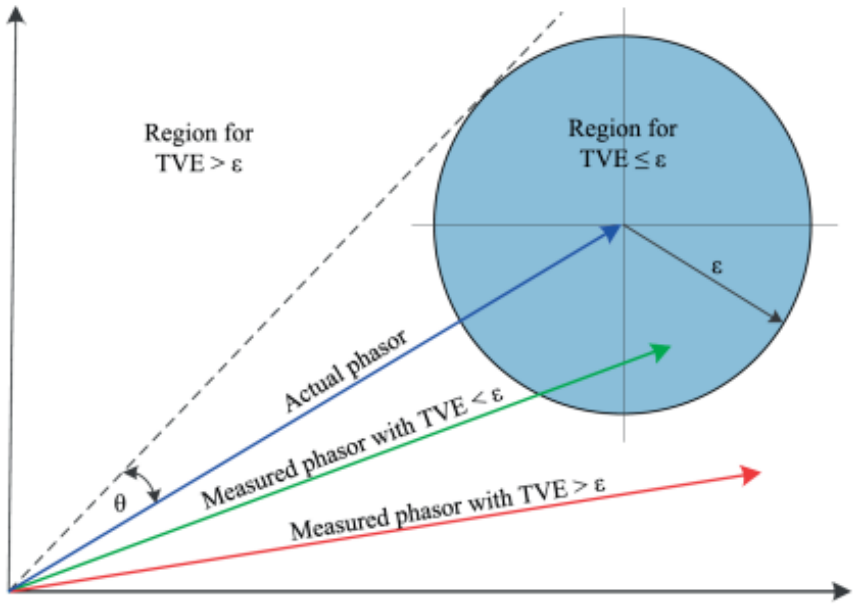

Figure 2.4: Graphical representation of the TVE. Based on IEEE C37.118

2.4 Static(Steady-state) Compliance

In order to reach our objective for this project, we must accomplish different tests(calculation TVE percentage) for different sampling rates(1.8kHz and 5.4kHz) and also for different quantization resolutions (12-bit and 16-bit).

2.4.1 Steady-state Signal Frequency:

The frequency f in 2.1is varied from 45 Hz to 55 Hz with a step resolution of 0.2 Hz while all other quantities are kept constant. The maximum values of percentage TVE are shown in the graphs below. The frequency signal deviates from the nominal frequency. This phasor rotation (variable phase) should be considered when evaluating TVE as per [1]; the PMU signal frequency TVE compliance is satisfied as the maximum TVE is less than 1% for frequencies between 45 Hz and 55 Hz for both 1.8 kHz and 5.4 kHz sampling rates at different quantization resolutions (12 bit , 16 bit):

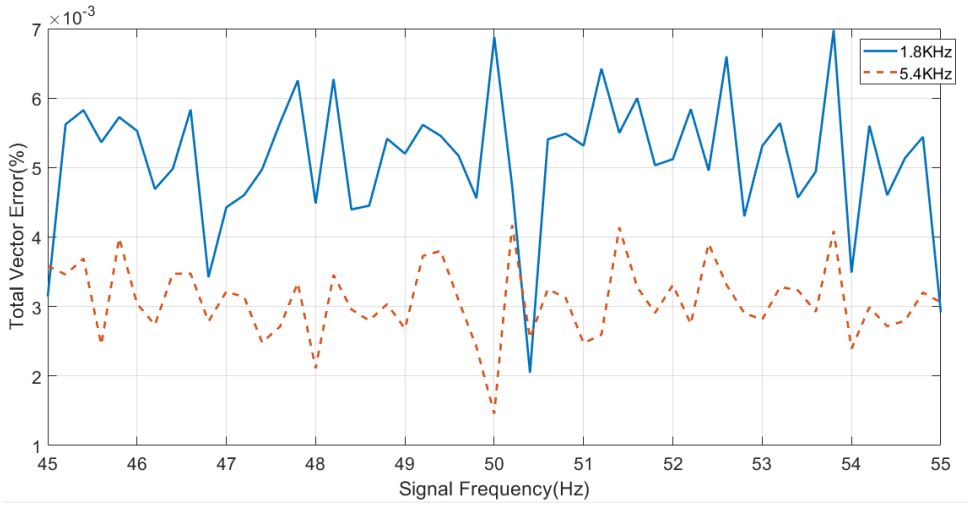

Figure 2.5: TVE of Steady-state signal frequency response at 12-bit resolution for 1.8Khz and 5.4kHZ sampling rate.

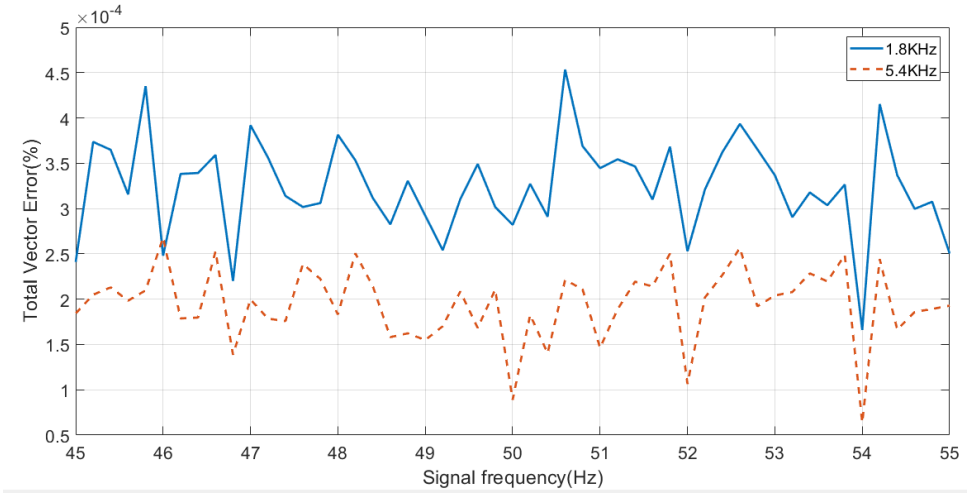

Figure 2.6: TVE of Steady-state signal frequency response at 16-bit resolution 1.8Khz and 5.4kHZ sampling rate.

It is shown clearly in figures 2.5 and 2.6 that the percentage TVE is decreased when the sampling rate and/or resolution of the A/D converter are increased from 1.8KHz to 5.4KHz and from 12bit to 16bit respectively .

2.4.2 Steady-state Signal Magnitude: Voltage

According to IEC/IEEE 60255-118-1:2018, the magnitude per unit (pu) X_m in 2.1 is being varied from 10% to 120% with a step variation of 0.05pu while all other quantities are kept constant.

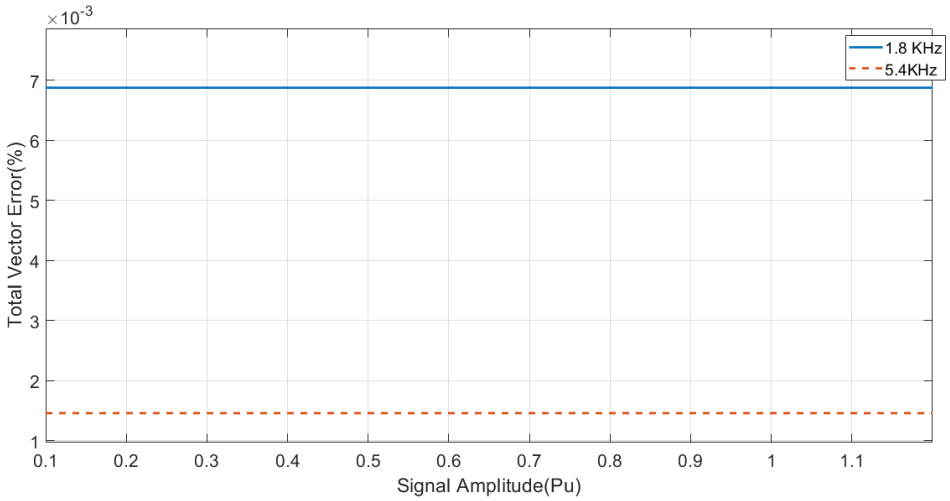

Figure 2.7: TVE of Steady-state signal magnitude response for voltage at 12-bit resolution for 1.8 kHz and 5.4kHZ sampling rates.

Figures 2.7 and 2.8 represent the max values of percentage TVE .The PMU voltage signal magnitude TVE compliance is satisfied as the maximum TVE is less than 1% for both 1.8 kHz and 5.4 kHz sampling rates at different quantization resolutions (12 bit and 16 bit):

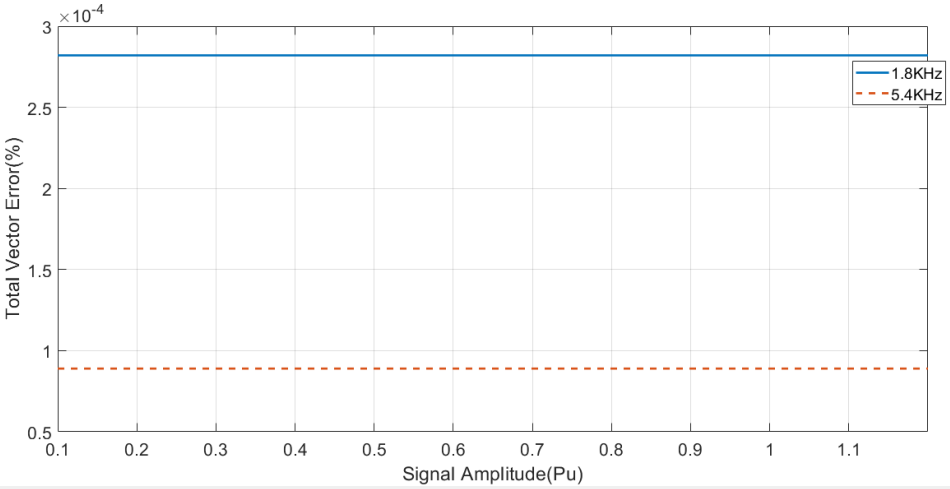

Figure 2.8: TVE of Steady-state signal magnitude response for voltage at 16-bit resolution for 1.8Khz and 5.4kHZ sampling rate.

It is shown clearly in figures. 2.7 and 2.8 that the percentage TVE is decreased when the sampling rate and/or resolution of the A/D converter are increased from 1.8KHz to 5.4KHz and 12bit to 16bit respectively .

2.4.3 Steady-state Signal Magnitude: Current

The current signal magnitude X_m in 2.1 is varied from 0.1 to 2 (pu) with a step resolution of 0.025pu while all other quantities are kept constant. Figures.2.9 and 2.10 show the max values of percentage TVE. The PMU current signal magnitude TVE compliance is satisfied as the maximum TVE is less than 1% for both 1.8 kHz and 5.4 KHz sampling rates at different quantization resolutions (12 bit, 16 bit):

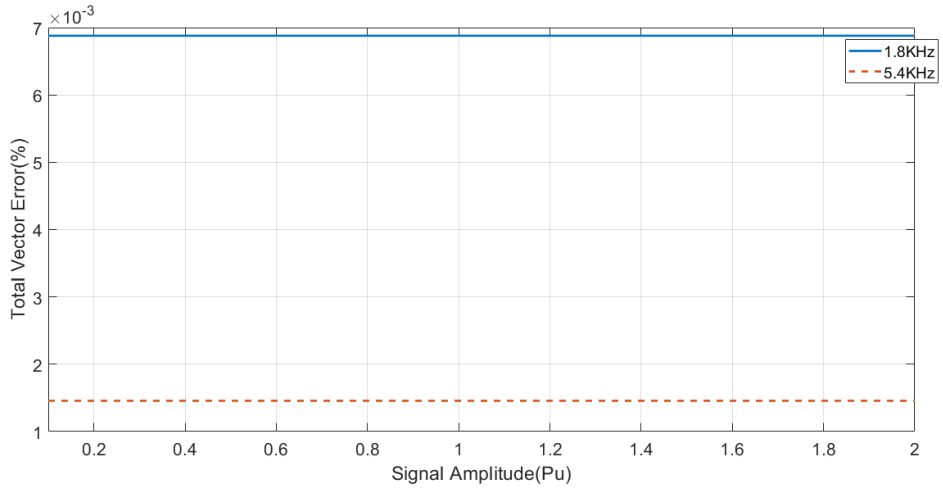

Figure 2.9: TVE of Steady-state signal magnitude response for current at 12-bit resolution for 1.8 kHz and 5.4Khz sampling rate.

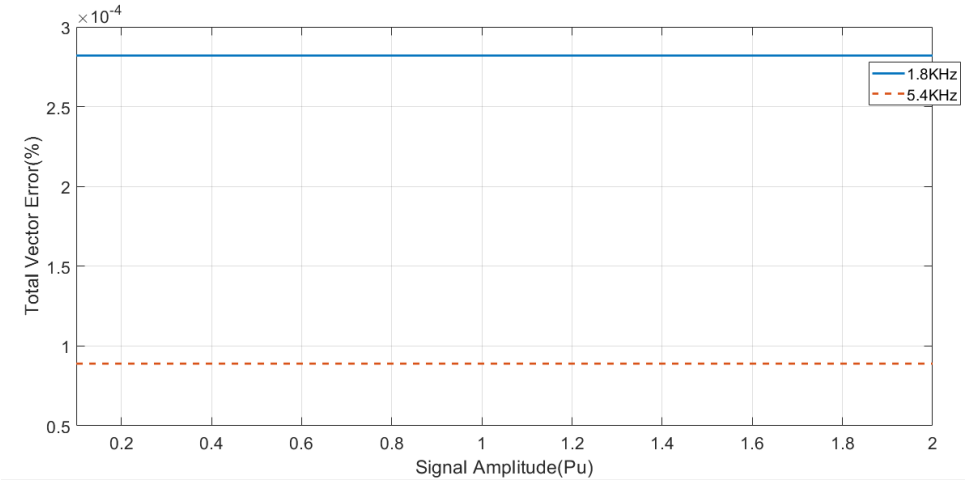

Figure 2.10: TVE of Steady-state signal magnitude response for current at 16-bit resolution for 1.8 kHz and 16Khz sampling rate.

It is shown clearly in figures. 2.9 and 2.10 that the percentage TVE is decreased when the sampling rate and/or resolution of the A/D converter are increased from 1.8KHz to 5.4KHz

and 12bit to 16bit respectively .

2.4.4 Steady-state Phase Angle:

The phase angle ϕ in 2.1is being varied from -180 to 180 degree with a step variation of 18^o while all other quantities are kept constant.

As it is shown in figures 2.11 and 2.12, the PMU current signal magnitude TVE compliance is satisfied as the maximum TVE is less than 1% for both 1.8 kHz and 5.4 Khz sampling rates at different quantization resolutions (12 bit, 16 bit):

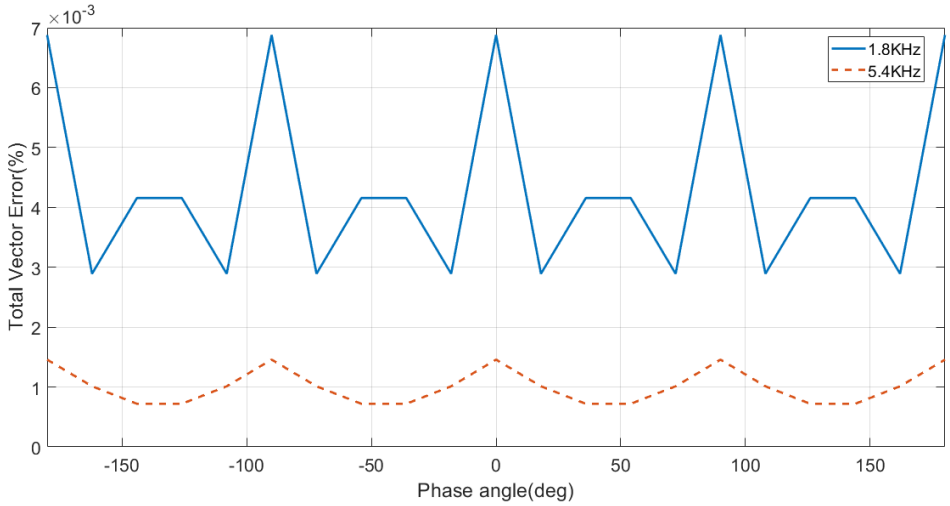

Figure 2.11: TVE of Steady-state phase angle response at 12-bit resolution for 1.8 kHz and 5.4 KHz sampling rates.

It is clearly shown in figures. 2.11 and 2.12 that the percentage TVE is decreased when the sampling rate and/or resolution of A/D converter are increased from 1.8KHz to 5.4KHz and 12bit to 16bit respectively .

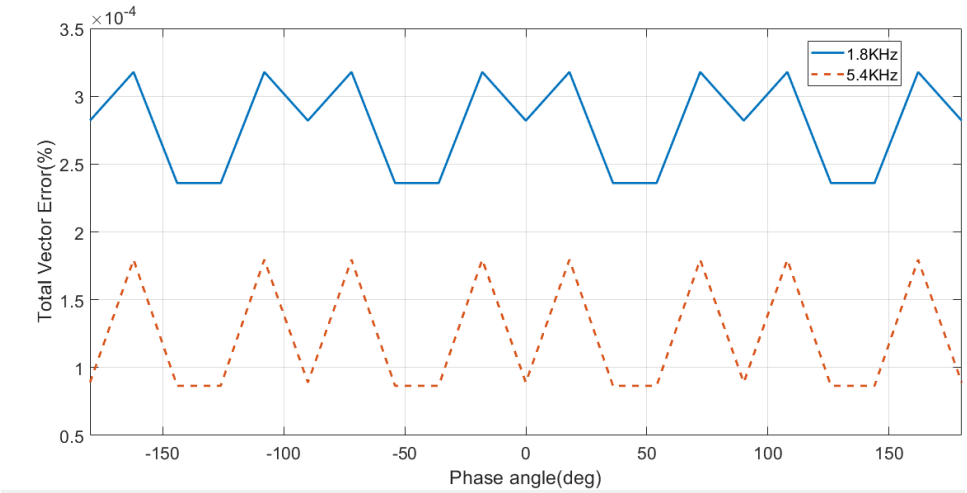

Figure 2.12: TVE of Steady-state phase angle response at 16-bit resolution; 1.8 kHz and 5.4 KHz sampling rate.

2.4.5 Steady-state Harmonic Distortion:

A 10% harmonic is introduced into the test signal where the equation 2.1 becomes:

$$x(t) = X_m cos(2\pi f_0 t + \phi) + 0.1 X_m \cos(2\pi f_0 k t + \phi_1) \tag{2.32}$$

The k parameter that represents the harmonic number is varied from 2 to 50 while all other quantities are kept constant. Figures. 2.13 and 2.14 show the maximum values of percentage TVE. The PMU harmonic distortion TVE compliance is satisfied as the maximum TVE is less than 1 % for a 10% harmonic for signals variation ranging between the 2nd and the 50th harmonic for both 1.8 kHz and 5.4 kHz sampling rates at different quantization resolution (12 bit , 16 bit).

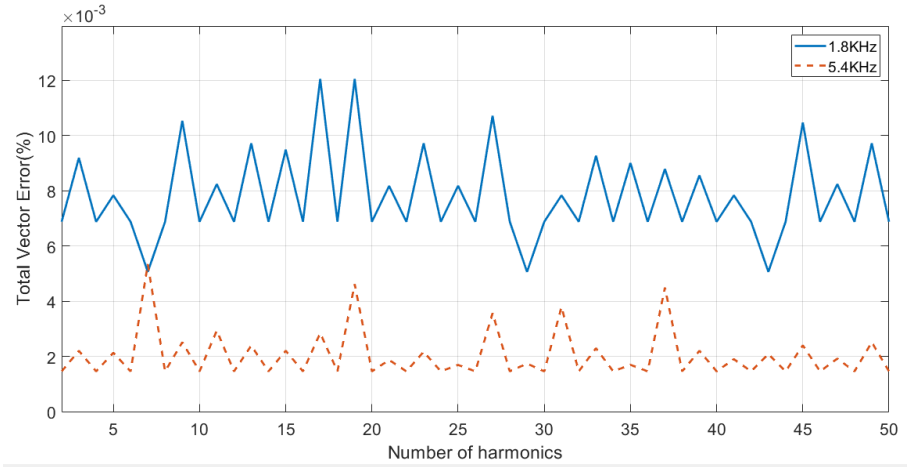

Figure 2.13: TVE of Steady-state harmonic distortion response at 12-bit resolution for 1.8 KHz and 5.4 KHz sampling rates.

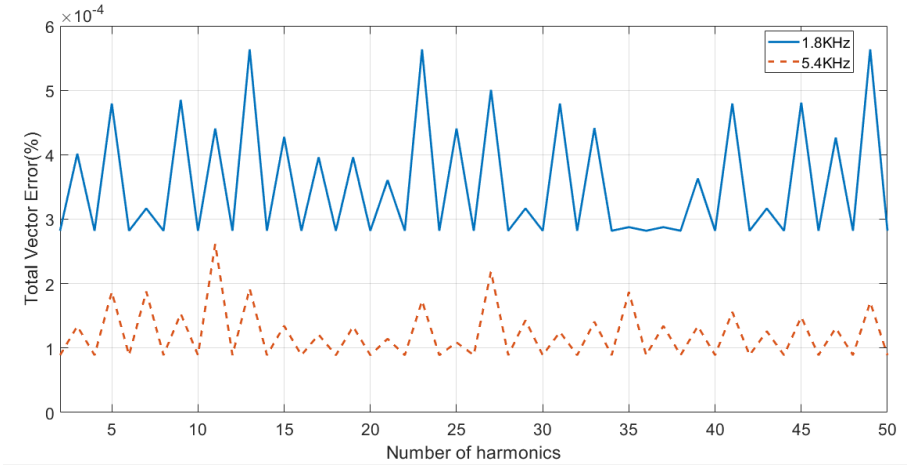

Figure 2.14: TVE of Steady-state harmonic distortion response at 16-bit resolution for 1.8 kHz and 5.4 KHz samping rates.

It is shown clearly in figures. 2.13 and 2.14 that the percentage TVE is decreased when the sampling rate and/or resolution of A/D converter are increased from 1.8KHz to 5.4KHz and 12bit to 16bit respectively .

2.4.6 Steady-state Out-of-Band Interference

A 10% out-of-band interference is introduced into the test signal

$$x(t) = X_m cos(2\pi f_0 t + \phi) + 0.1 X_m cos(2\pi f_{0b} t + \phi) \tag{2.33}$$

The frequency of an interference (out of band) signal, $f_{ob}$is varied from 10 Hz to $2f_0$ which is 100 Hz while all other quantities are kept constant. The PMU harmonic distortion TVE compliance is not satisfied as the maximum TVE is greater than 1 % for a 10% out of band interference for signals for both 1.8 kHz and 5.4 Khz sampling rates at different quantization resolution (12 bit , 16 bit): In figure. 2.15 the percentage TVE remains the same when the

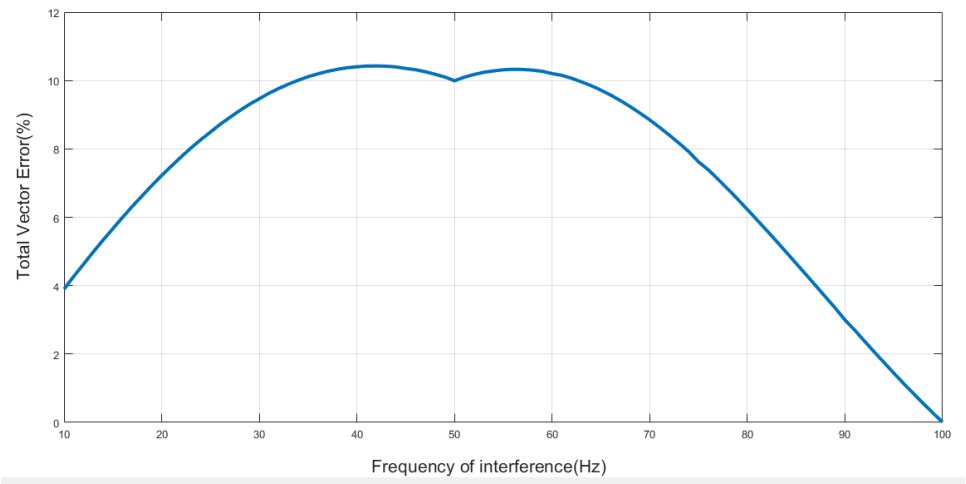

Figure 2.15: Steady-state 10% out of band interference response.

sampling rate and/or resolution of A/D converter are increased from 1.8KHz to 5.4KHz and 12bit to 16bit respectively.

2.4.7 Comments of different resolutions:

The percentage TVE is being calculated for different quantization levels (12,14 and 16 bits) at 1.8k sampling rate for all of steady state signal frequency, voltage and current Signal Magnitude, phase angle and harmonic distortion.

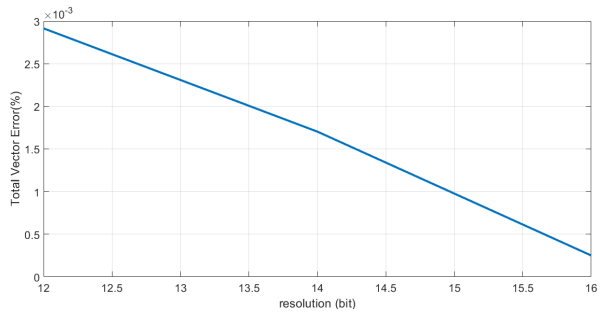

Figure 2.16: Frequency TVEs due to quantization resolution.

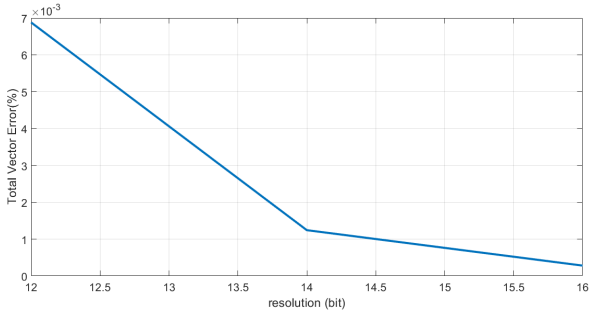

Figure 2.17: Magnitude of Current and voltage TVEs due to quantization resolution.

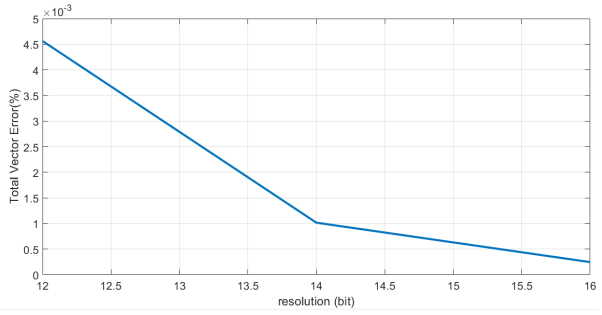

Figure 2.18: Phase angle TVEs due to quantization resolution.

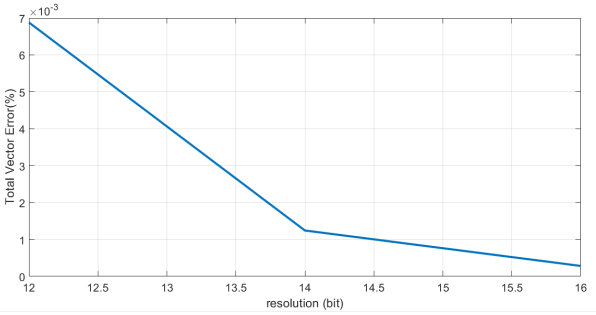

Figure 2.19: Harmonic distortion TVEs due to quantization resolution.

Figures 2.16, 2.17, 2.18 and 2.19 show clearly that the relationship between the TVE and quantization resolution is inversely proportional; as the resolution increases, the TVE decreases,as well as for the sampling rates and quantization resolution (12 bit , 16 bit): Figures 2.20, 2.21, 2.22 and 2.23 demonstrate that.

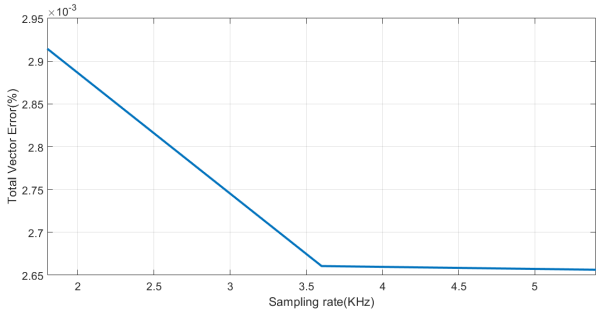

Figure 2.20: Frequency TVEs due to quantization resolution.

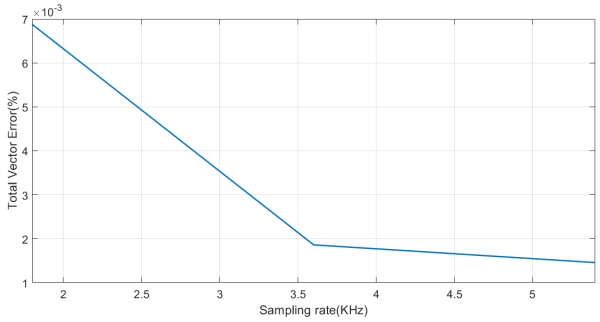

Figure 2.21: magnitude of Current and voltage TVEs due to quantization resolution.

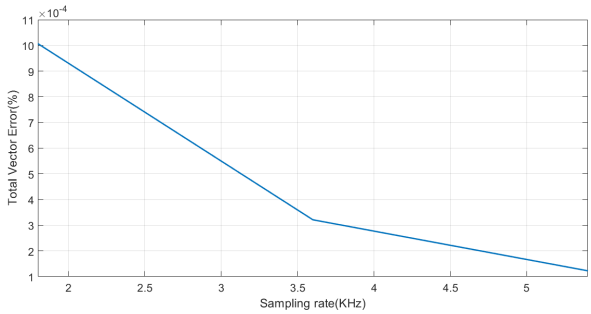

Figure 2.22: Phase angle TVEs due to quantization resolution.

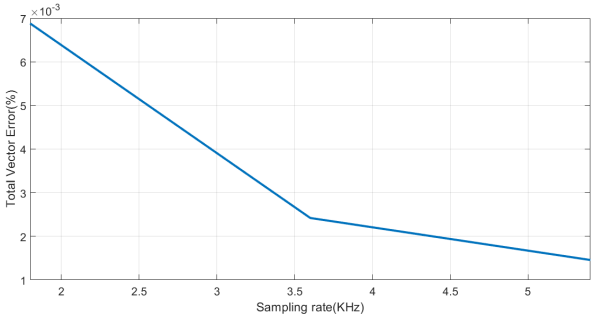

Figure 2.23: Harmonic distortion TVEs due to quantization resolution.

2.5 Dynamic compliance

Dynamic conditions are defined in [1] which includes the evaluation measurement of linear system frequency ramp and step response of magnitude and phase angle .

2.5.1 Measurement Bandwidth

The synchrophasor measurement bandwidth shall be determined as mentioned in [14] by replacing the input signal with sinusoidal amplitude and phase modulation. This shall be done by inserting sinusoidal amplitude and phase angle to the original voltage and current signals . Mathematically, the input signals may be represented by Equation2.34

$$x_1 = x_m[1 + k_x cos(\omega t)].cos[\omega_0 t + k_a cos(\omega t - \pi)] \tag{2.34}$$

where :
x_m is the amplitude of the input signal
ω_0 is the nominal power system frequency
ω is the modulation frequency in radians/s

k_x is the amplitude modulation factor
k_a is the phase angle modulation factor.

According to [1], the modulation frequency must be varied in steps of 0.2 Hz or less over the range [0.1 to 5] Hz, while the magnitude and phase angle modulation levels, k_x and k_a, must be kept at 10%.The TVE %, FE, and RFE shall be measured over at least two full modulation cycles. The maximum and mean values of percentage TVE are shown in Figure2.24.

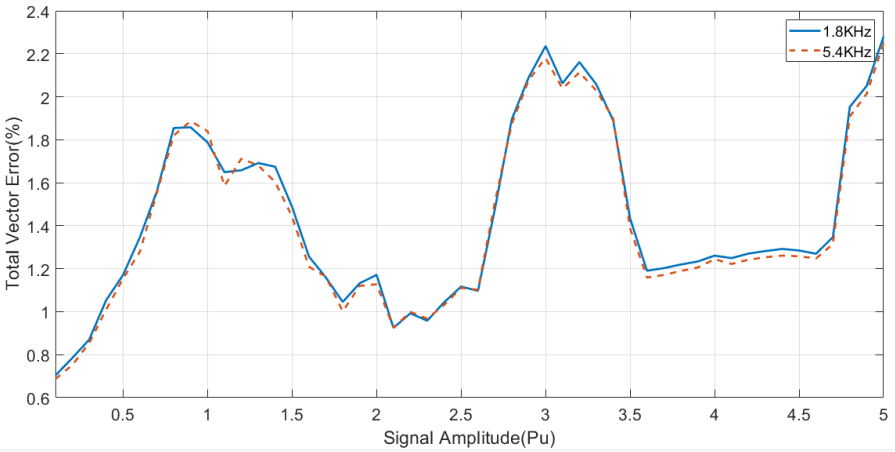

Figure 2.24: Magnitude and phase angle modulation response with sampling rates of 1.8KHz and 5.4KHz.

Comments The PMU satisfies measurement bandwidth TVE compliance up to a modulation frequency of 5 Hz as maximum TVE is less than 3%. Thus, the PMU satisfies both P and M class compliance.

2.5.2 Ramp of System Frequency

Measurement performance during system frequency change shall be tested according to [1] with linear ramp of the system frequency aplied to input signals (voltages and currents). Mathematically the input signals may be represented by Equation 2.35

$$X(t) = X_m cos(\omega_0 t + \pi R_f t^2) \tag{2.35}$$

where X_m is the amplitude of the input signal, ω_0 is the nominal power system frequency, and rf=($\frac{df}{dt}$) is the frequency ramp rate in Hz/s in which is of a fixed value in this equation.

The signal frequency ramp rate, R_f is varied from negative ramp (−1.0 Hz/s) to positive ramp (+1.0 Hz/s) while the ramp range is from 45 Hz to 55 Hz. The maximum and mean values of percentage TVE are shown in Fig.2.25.

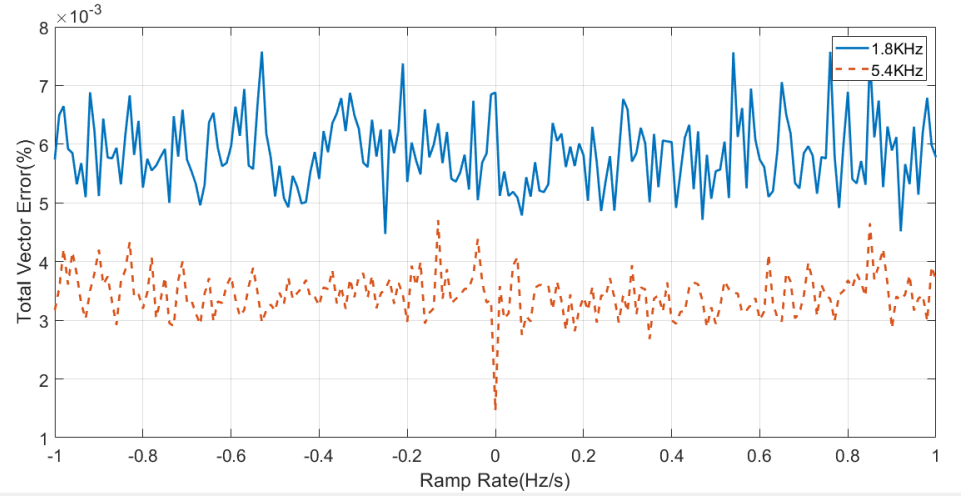

Figure 2.25: Linear frequency ramp response with 1.8kHz and 5.4 kHz sampling rate.

Comments

The graph in fig2.25 shows that IEC/IEEE 60255-118-1 frequency ramp compliance are verified for both P class and M class as the maximum TVE is less than1% for ramp rate between −1.0 Hz/s and +1.0 Hz/s while the ramp range is from 45 Hz to 55 Hz.

2.5.3 Step Response

Step responses allow testing the PMU's response to a sudden input change, which might occur during load switching and faults. As it is mentioned in IEC/IEEE 60255-118-1.2018.standards, only magnitude and phase angle parameters will be taken under test. Positive and negative steps of 10% magnitude and 10% phase angle are included. The step is started by a signal at a specific moment, allowing the response time, delay time, and maximum overshoot/undershoot to be determined.A unit step function u(t) is applied to the input signal magnitude and phase angle and it is represented in (2.36) as:

$$x(t) = X_m[1 + k_x.u(t)].cos[\omega_0 t + \phi_0 + k_a u(t)] \tag{2.36}$$

The magnitude step size,k_x and the phase angle step size, k_x are taken as -0.1 and +0.1 for negative and positive steps respectively. Figures 2.26, 2.27, 2.28, 2.29 represents magnitude positive step change different parameters responses(signal, amplitude, phase angle and TVE).

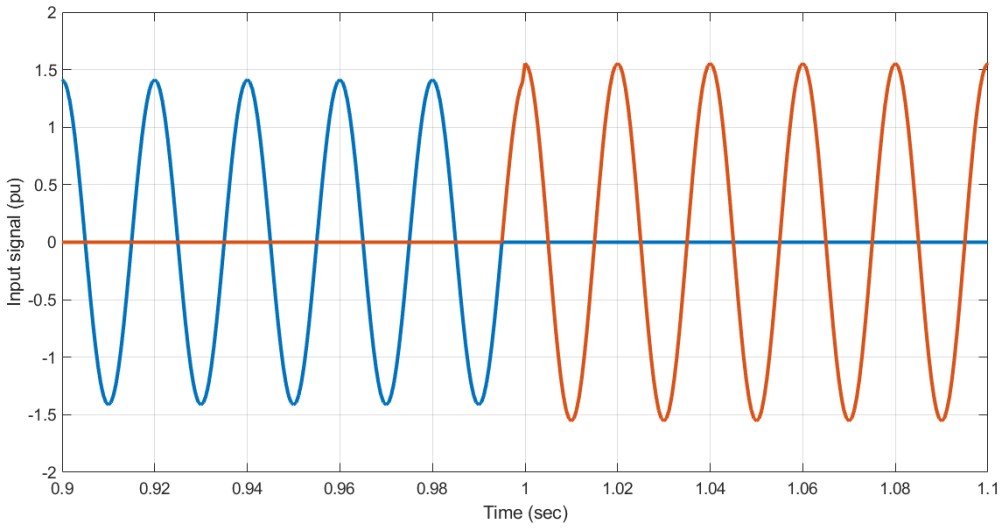

Figure 2.26: Input signal waveform during magnitude step change.

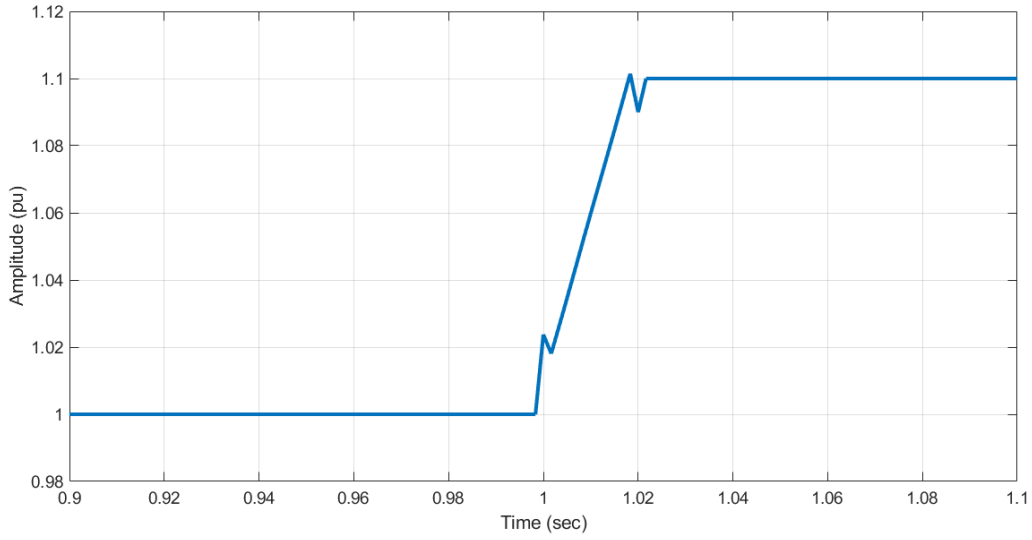

Figure 2.27: Signal amplitude response during magnitude step change.

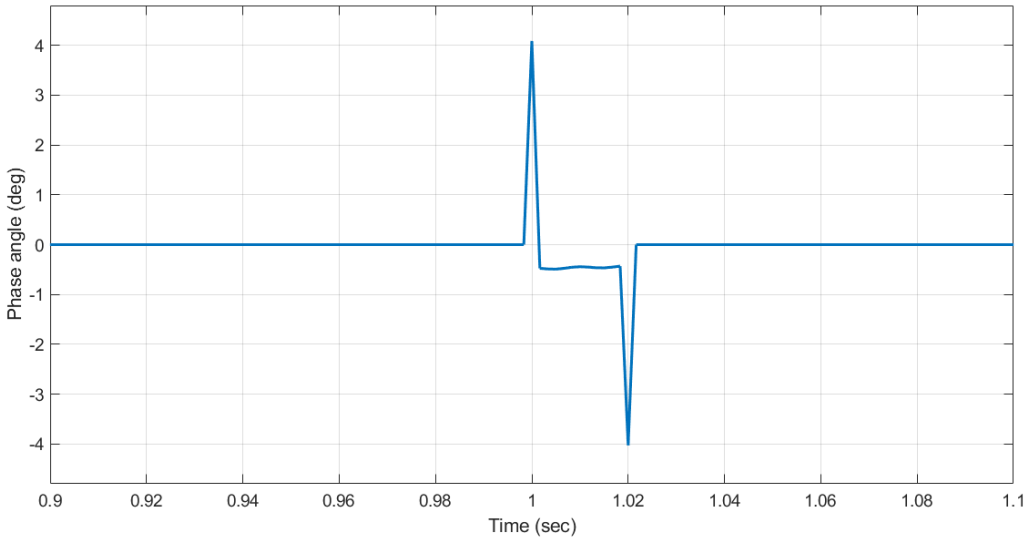

Figure 2.28: Signal phase angle response during magnitude step change.

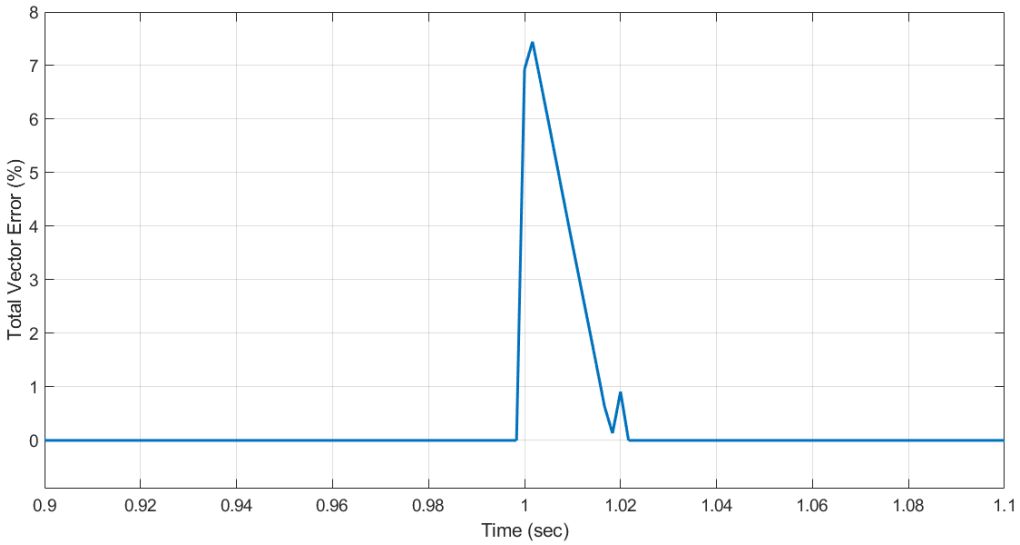

Figure 2.29: Percentage TVE of magnitude step change.

For phase angle step change, the figures below (2.30,2.31, 2.32, 2.33) demonstrates the effect of the step change on each of input test signal, signal amplitude, phase angle and percentage TVE.

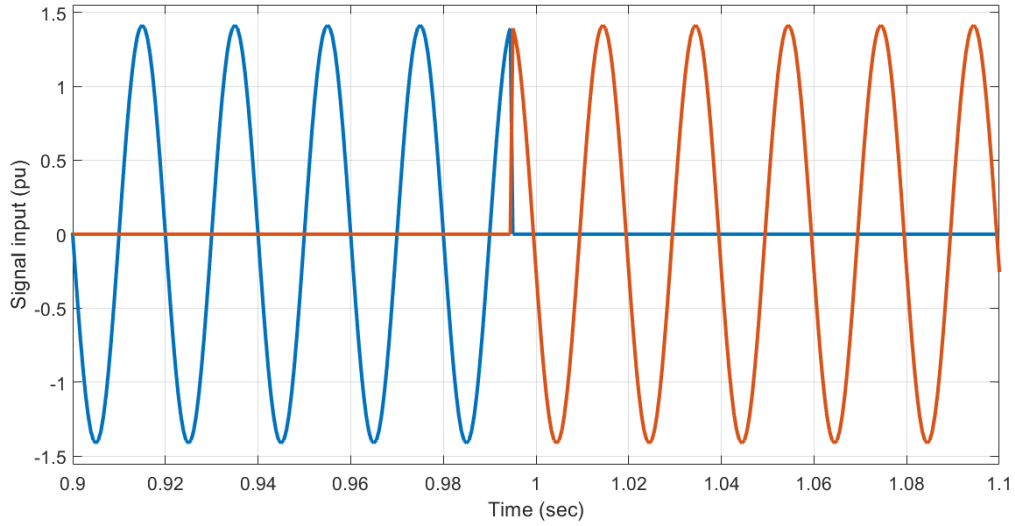

Figure 2.30: Input signal waveform during phase angle step change.

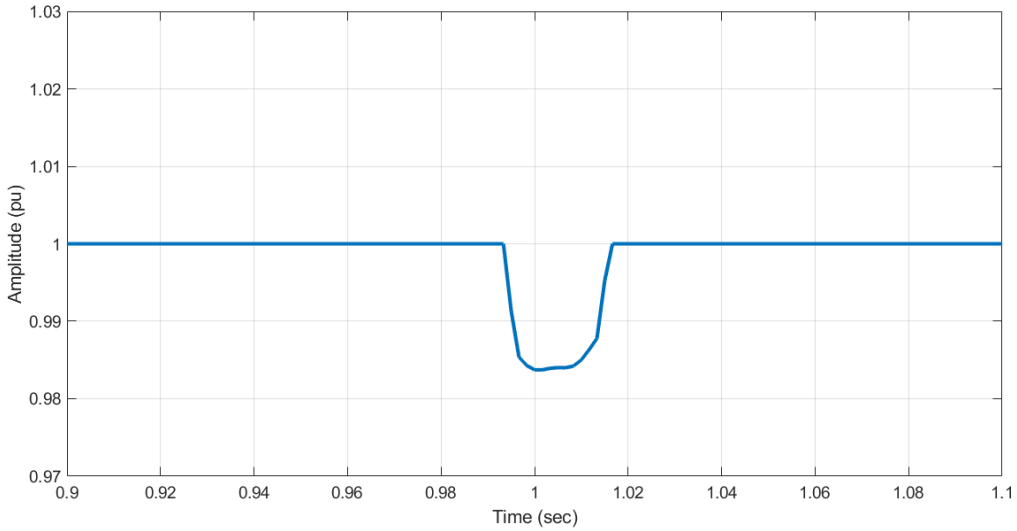

Figure 2.31: Signal amplitude response during phase angle step change.

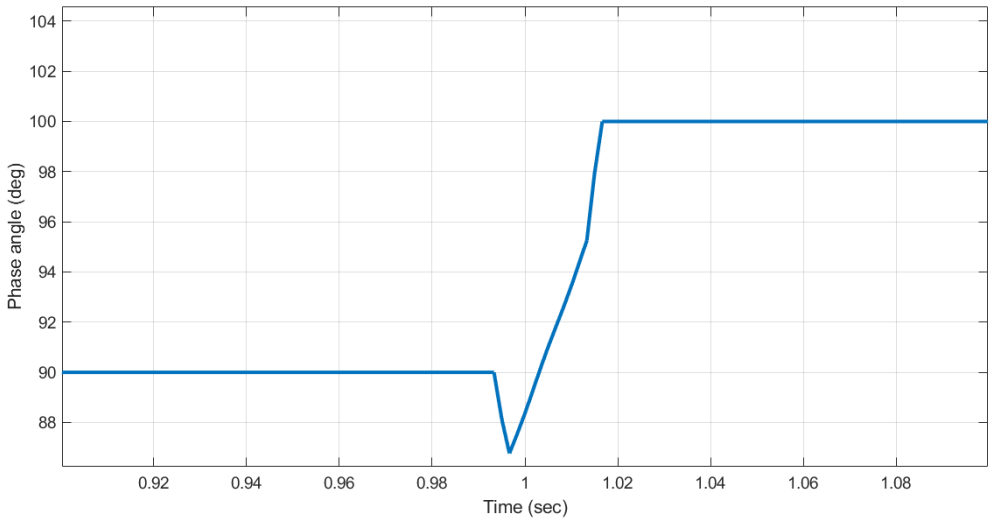

Figure 2.32: Signal phase angle response during phase angle step change.

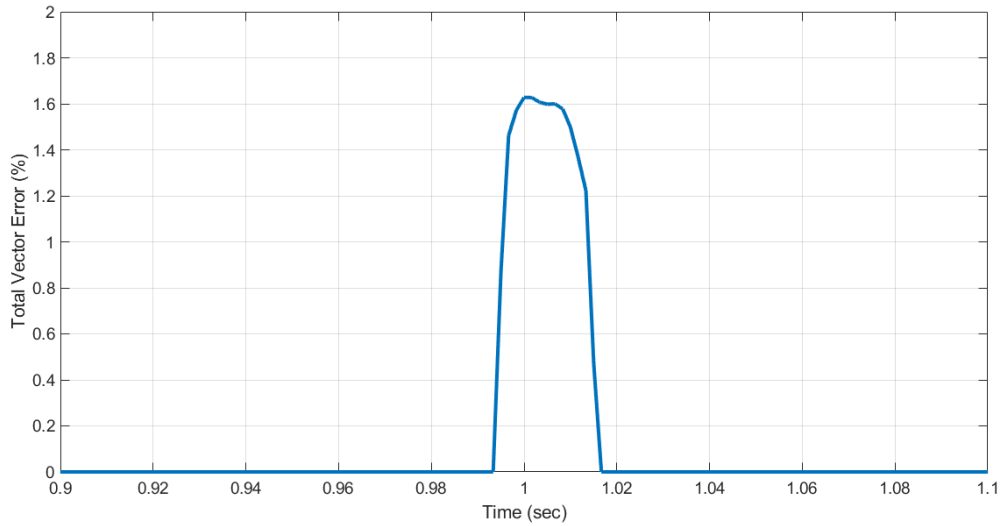

Figure 2.33: Percentage TVE of phase angle step change.

Comments

- Percentage overshoot
  According to IEC/IEEE standards, maximum overshoot must not exceed 5% for M class and 10% for P class, we get 0.015 PU which is 1.5% overshoot.

- Time delay
  It is defined as the difference between 50% of the final value time and the starting time of step change, which is recommended to be less than 5 ms. In our case, delay time is equal to 13 ms for phase step change and 8 ms for magnitude step change, which is a little bit higher than the required value. This can be explained by the disadvantage of using SDFT only for controlling frequency, which may suffer from different disturbances that cause some transient phasors.

- Total vector error
  For dynamic state, TVE must not exceed 1%, figures 2.33 and 2.29 shows that tve maximum level is not exceeded only for step change interval.

2.6 Conclusion

This chapter was intended to verify the compatibility of phasor estimation algorithms that are defined at the beginning of the chapter with IEEE Std. C37.118 compliance for both steady state and dynamic state. In order to achieve our objectives for this project, estimation tests were done for different sampling rates and different quantization resolutions. The results of different tests show that almost all of the IEC/IEEE standards constraints have been respected, which proves the efficiency of the DFT estimation algorithm. It is also concluded that the increasing of sampling rate and quantization resolution reduce the total vector error for different parameters by a remarkable amount, leading to the improvement of PMU efficiency.

Chapter 3

LabVIEW PC based PMU:

3.1 Introduction:

Chapter 2 covered the basic design as well as the (simulation) implementation of the PMU and the testing with different sampling rates and resolutions with the DFT algorithm using MATLAB . In this chapter, we will show how the phasor estimator is generated using an algorithm and how the calculations are carried out using LABVIEW software. The PMU device was then tested, which required evaluating the PMU's performance through several tests, getting results, and making inferences based on those results.

3.2 What is LabVIEW?

For applications requiring test, measurement, and control with quick access to hardware and data insights, LabVIEW is systems engineering software. The LabVIEW programming environment simplifies hardware integration for engineering applications so that you have a consistent way to acquire data from NI and third-party hardware. LabVIEW reduces the complexity of programming so you can focus on your unique engineering problems. LabVIEW enables you to immediately visualize results with built-in, drag-and-drop engineering user interface creation and integrated data viewers. To turn your acquired data into real business results, you can develop algorithms for data analysis and advanced control with included math and signal processing IP or reuse your own libraries from a variety of tools. To ensure compatibility with other engineering tools, LabVIEW can interoperate with and reuse libraries from other software and open-source languages. A VI consists of two different panels (Figure3.1): a graphical programming panel (or the block diagram), and a visual front panel. For engineers, LabVIEW makes it possible to bring information from the outside world into a computer, make decisions based on the acquired data, and send computed results back into the world to control the way a piece of equipment operates.[23]

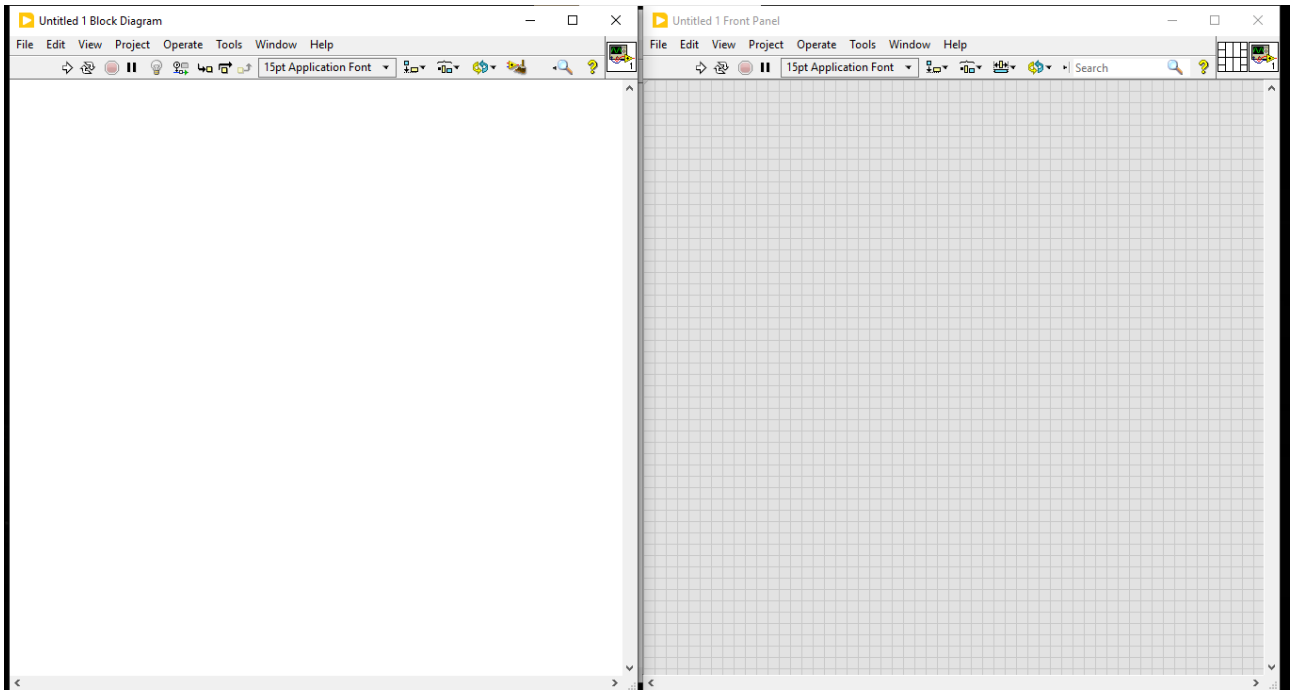

Figure 3.1: Block Diagram and Front Panel for VI.

3.3 LABVIEW MODELLING OF PMU:

3.4 Simulation of the phasor estimator:

- The non-recursive algorithm

The input signal for the non-recursive algorithm was created using library VI as an analog signal and then converted to a discrete signal using A/D (Analog to Digital Converter) VI. Here, a 12-sample data window is considered. A user-defined VI must be created to calculate the Fourier coefficient of the data samples. Suitable arithmetic operations are performed to estimate the phasor for the first data window. After phasor computation, the complex term is transformed into polar form and shown as an output. This algorithm is performed for each consecutive data sample. As a newer estimate of the phasor is conducted, the phasor rotates anticlockwise by an angle θ due to the delay of each sample by one sampling angle. Figure 3.2 shows the created non-recursive LABVIEW model.

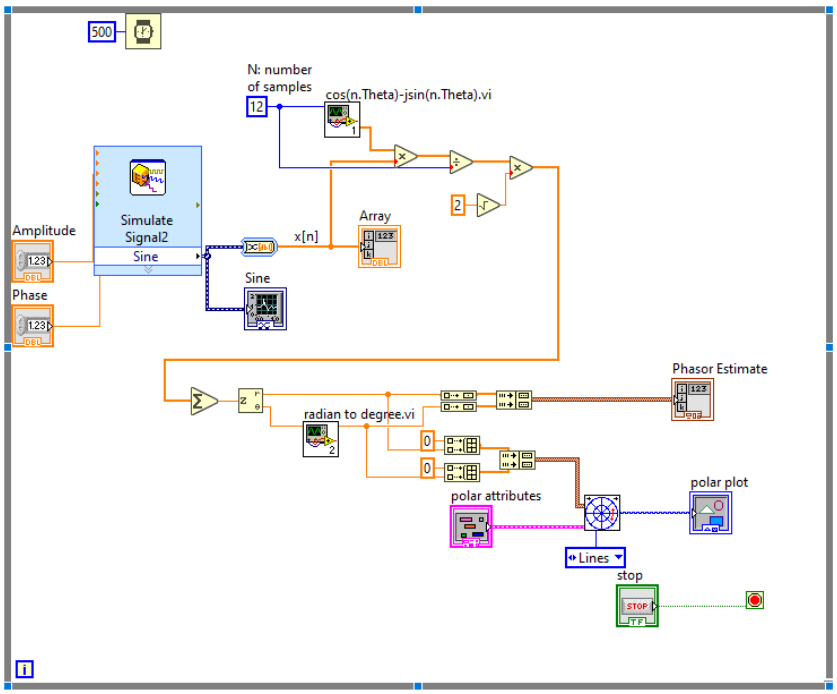

Figure 3.2: block diagram for The non-recursive algorithm.

- The recursive algorithm

A phasor estimate acquired across a data window, ideally using a non-recursive approach, is required for the recursive process.In the case studies shown below, the above algorithm is employed to construct the initial phasor estimate. The recursive algorithm is utilized after obtaining the phasor for one data window.When a phasor estimate is obtained for the (N+r-1)th sample, (N+r) the sample is compared with r the sample using suitable mathematical operands provided in the standard library. The difference in the sample value dictates the updation of new estimates of phasor using Equation 2.12.

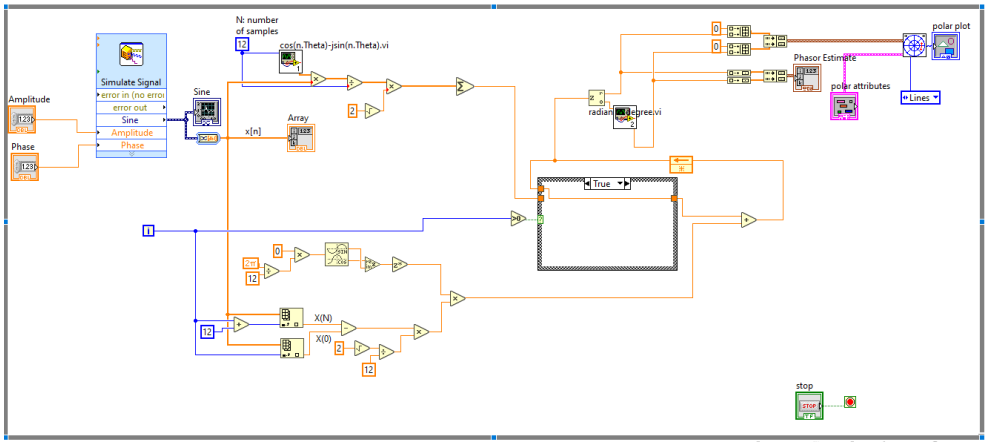

Figure 3.3: The recursive labVIEW model (true case).

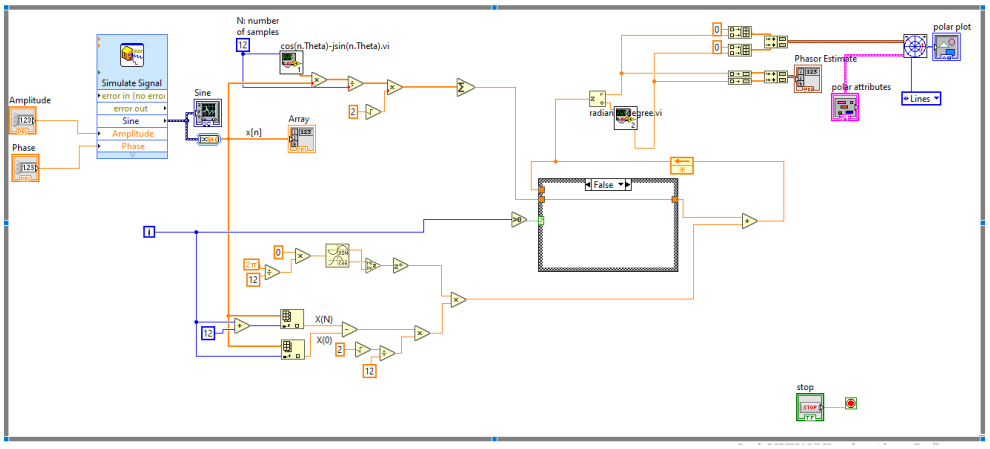

Figure 3.4: The recursive labVIEW model (false case).

3.5 Testing and results of the simulation:

A signal of $100cos(100\pi t + \pi/4)$ is taken for the result validation with the mathematical analysis. Twelve samples per cycle are taken by the A/D converter so the sampling time becomes $\frac{1}{12\times 50} = \frac{1}{600} second$.

Table 3.1: Phasor estimation for recursive and non-recursive algorithm

Sample number	Sample Xn	Recursive		Non-recursive	
		Magnitude	Angle	Magnitude	Angle
0	70.7107	/	/	/	/
1	25.8819	/	/	/	/
2	-25.8819	/	/	/	/
3	-70.7107	/	/	/	/
4	-96.5926	/	/	/	/
5	-96.5926	/	/	/	/
6	-70.7107	/	/	/	/
7	-25.8819	/	/	/	/
8	25.8819	/	/	/	/
9	70.7107	/	/	/	/
10	96.5926	/	/	/	/
11	96.5926	/	/	/	/
12	70.7107	70.7107	45°	70.7107	45°
13	25.8819	70.7107	45°	70.7107	75°
14	-25.8819	70.7107	45°	70.7107	105°
15	-70.7107	70.7107	45°	70.7107	135°
16	96.5926	70.7107	45°	70.7107	165°
17	-96.5926	70.7107	45°	70.7107	195°
18	-70.7107	70.7107	45°	70.7107	225°
19	25.8819	70.7107	45°	70.7107	255°

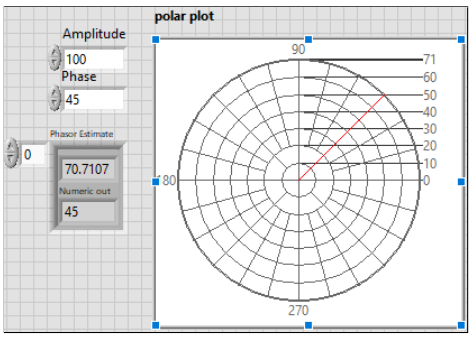

Figure 3.5: Polar plot for first window for the non-recursive algorithm.

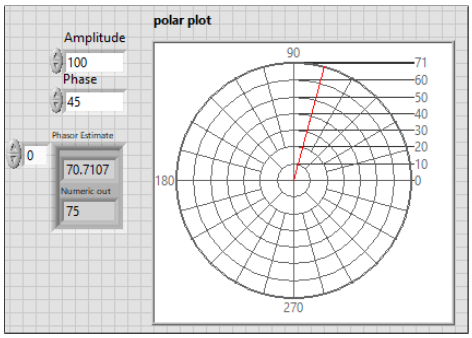

Figure 3.6: Polar plot for second window for non-recursive algorithm.

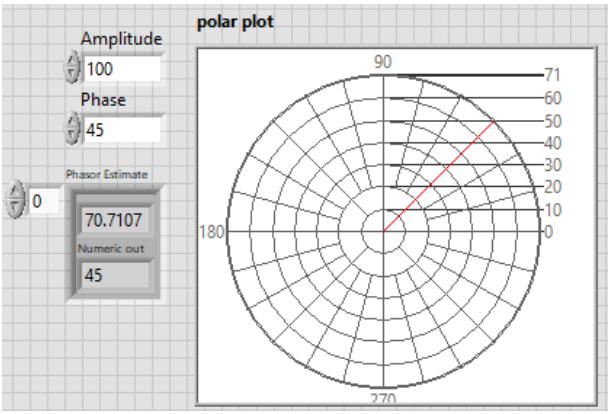

Figure 3.7: Phasor of the recursive algorithm.

We notice that for the non-recursive estimate from table 3.1 and on figures 3.5 and 3.6, the magnitude is fixed but the phase increases by a constant amount of 30^o ,on the other hand, with the recursive estimate in table 3.1 and figure 3.7 both the magnitude and phase are fixed.

3.6 Conclusion

The non-recursive and recursive DFT-based approaches are used to model the Synchrophasor Unit or the PMU using NI LabVIEW software. The results obtained from the PMU model are found to be similar when compared with the mathematical analysis for phasor calculation. This can provide useful information for future real-time PMU implementation in a smart grid prototype.

General Conclusion

First, we implemented a DFT measurement algorithm to estimate the phasor magnitude and phase angle at nominal frequency. the sampling frequency and the quantization error effects have been included in this phasor estimation. The smart dft algorithm complements the dft to estimate the phasors at off-nominal frequency is implemented. These combined algorithms are used to estimate different power network parameters as defined in the standard of c37-118 (TVE, F, FE ,ROCOF.. etc) . The conformance test of the implemented algorithm with that of the standard has been carried out for the P-class requirements . The sampling frequency and quantization effect have been considered for both static and dynamic conformance tests. All parameters have been tested as per the standard of c37-118.[14].

This has led us to generate different test signals provided by the standard, which may be considered as a reference of known parameters(magnitude, phase angle ,phasors)and use our implemented algorithm to measure the test signal parameters . The error then can be performed between the measured and the reference one (the generated reference test signal). The simulation tests have been carried out for different sampling frequencies and quantization resolutions.
The test results show that increasing the sampling frequency and quantization resolution improves the accuracy of the measured algorithm. Hence, a frequency of more than 5.4KHz and 16 bits ADC or higher may satisfy the requirements of the standard .
Labview has been selected to implement the micro pmu. A non-real-time LabVIEW project is designed to implement the measurement algorithm . This program also provides waveform signals to test the pmu measurement algorithm at nominal frequency, and good results are obtained .

For future work, we suggest using a data acquisition board such as the NI PCI 6021 or other boards with higher specifications. and a signal conditioning circuit to acquire the voltage and current signals derived from the line power network as described in Chapter 1 . A real-time labview program must also be designed implementing the developed algorithm(recursive

non-recursive,smart DFT) using the sampling frequency as requested from our work to implement the designed micro PMU . A hardware real-time conformance test using the developed micro PMU and a testing device such as the "omicron CMC356" . Finally The standard conformant test has to be carried out .

Bibliography

[1] Kenneth E Martin. Synchrophasor measurements under the ieee standard c37. 118.1-2011 with amendment c37. 118.1 a. *IEEE Transactions on Power Delivery*, 30(3):1514–1522, 2015.

[2] Chetan Mishra. *Optimal substation coverage for phasor measurement unit installations*. PhD thesis, Virginia Tech, 2012.

[3] Dave Schofield, Francisco Gonzalez-Longatt, and Dimitar Bogdanov. Design and implementation of a low-cost phasor measurement unit: A comprehensive review. In *2018 Seventh Balkan Conference on Lighting (BalkanLight)*, pages 1–6. IEEE, 2018.

[4] Harvey Lehpamer. *Introduction to power utility communications*. Artech House, 2016.

[5] Arun G Phadke, James S Thorp, and M G Adamiak. A new measurement technique for tracking voltage phasors, local system frequency, and rate of change of frequency. *IEEE transactions on power apparatus and systems*, (5):1025–1038, 1983.

[6] Arun G Phadke and James S Thorp. *Synchronized phasor measurements and their applications*, volume 1. Springer, 2008.

[7] Mahesh K Penshanwar, Minakshi Gavande, and MFA R Satarkar. Phasor measurement unit technology and its applications-a review. In *2015 International Conference on Energy Systems and Applications*, pages 318–323. IEEE, 2015.

[8] Abderrahmane Ouadi. *Power system protection improvement using wide area synchrophasor measurements*. PhD thesis, 2015.

[9] Thomas Kugelstadt. Chapter 16: Active filter design techniques. *Texas Instruments, Application Report SLOA088*, 2008.

[10] JE Ffowcs Williams, I Roebuck, and CF Ross. Anti-phase noise reduction. *Physics in Technology*, 16(1):19, 1985.

[11] Takao Waho. *Introduction to Analog-to-Digital Converters Principles and Circuit Implementation*, pages i–xxviii. 2019.

[12] Fred Taylor. *Data Conversion and Quantization*, pages 29–39. 2012.

[13] Power System Relaying Committee et al. Ieee std c37. 118ˆ tm-2005 (revision of ieee std 1344ˆ tm-1995) ieee standard for synehrophasors for power systems, 2006.

[14] Ieee/iec international standard - measuring relays and protection equipment - part 118-1: Synchrophasor for power systems - measurements. *IEC/IEEE 60255-118-1:2018*, pages 1–78, 2018.

[15] Jian Chen. *Accurate frequency estimation with phasor angles*. PhD thesis, Virginia Tech, 1994.

[16] Adly A Girgis and TL Daniel Hwang. Optimal estimation of voltage phasors and frequency deviation using linear and non-linear kalman filtering: theory and limitations. *IEEE Transactions on Power Apparatus and Systems*, (10):2943–2951, 1984.

[17] Arun G Phadke, James S Thorp, and M G Adamiak. A new measurement technique for tracking voltage phasors, local system frequency, and rate of change of frequency. *IEEE transactions on power apparatus and systems*, (5):135–145, 1983.

[18] KE Martin, D Hamai, MG Adamiak, S Anderson, M Begovic, G Benmouyal, G Brunello, J Burger, JY Cai, B Dickerson, et al. Exploring the ieee standard c37. 118–2005 synchrophasors for power systems. *IEEE transactions on power delivery*, 23(4):1805–1811, 2008.

[19] Adly A Girgis and Fredric M Ham. A new fft-based digital frequency relay for load shedding. *IEEE Transactions on Power Apparatus and Systems*, (2):433–439, 1982.

[20] Arun G Phadke, James S Thorp, and M G Adamiak. A new measurement technique for tracking voltage phasors, local system frequency, and rate of change of frequency. *IEEE transactions on power apparatus and systems*, (5), 1983.

[21] Jun-Zhe Yang and Chih-Wen Liu. A precise calculation of power system frequency. *IEEE Transactions on Power Delivery*, 16(3):361–366, 2001.

[22] Dinesh Rangana Gurusinghe, Dean Ouellette, and Athula D Rajapakse. Implementation of smart dft-based pmu model in the real-time digital simulator. In *Conference: The International Conference on Power Systems Transients (IPST)*, 2017.

[23] Ronald W Larsen. *LabVIEW for engineers*. Pearson Higher Ed, 2011.